7th International Conference on
New Developments In Photodetection
Tours, France, June 30th to July 4th 2014
NDIP

Highlights of Poster Session "Blanc"

G.Collazuol
University of Padova and INFN

26 contributions: mostly about SiPM

- Devices / characterization / models (11)
- Timing (4)
- Applications (9)
- Other semiconductor Photo-det./systems (2)

Overview

Devices and properties of SiPM/SPAD

Devices and characterization
- SiPM devices/ new features
- VUV sensitivity and cryogenic characterization
- Characterization vs models / simulations

Timing properties
- intrinsic timing
- timing performances in applications

Systems – Applications using SiPM

Cherenkov (RICH, Cherenkov Telescope camera)
Scintillators (crystals, neutron det., plastics)

Other Photo-detectors / Systems

Devices and properties of SiPM/SPAD

Devices and characterization
- SiPM devices/ new features
- VUV sensitivity and cryogenic characterization
- Characterization vs models / simulations

Timing properties
- intrinsic timing
- timing performances in applications

Systems – Applications using SiPM

Cherenkov (RICH, Cherenkov Telescope camera)
Scintillators (crystals, neutron det., plastics)

Other Photo-detectors / Systems

Poster ID 10 – Florian Wiest (KETEK GmbH) et al

Recent Enhancements of the KETEK SiPM Device Performance with regard to PDE, Cross Talk and CMOS Compatibility

Subject: recent news from KETEK (about custom and CMOS process SiPMs)

Results: 1) improved optical trench insulation → reduced cross-talk
2) thicker epitaxial layer → wider PDE peak (extended toward green)
3) custom to CMOS technology transition ongoing: first results

Poster Session #1

1)

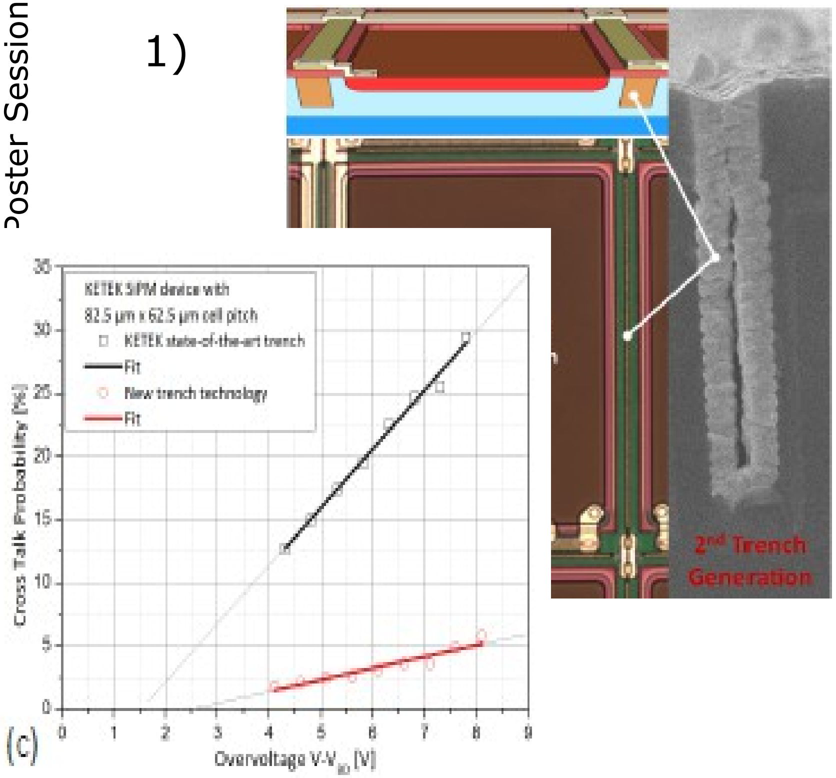

2)

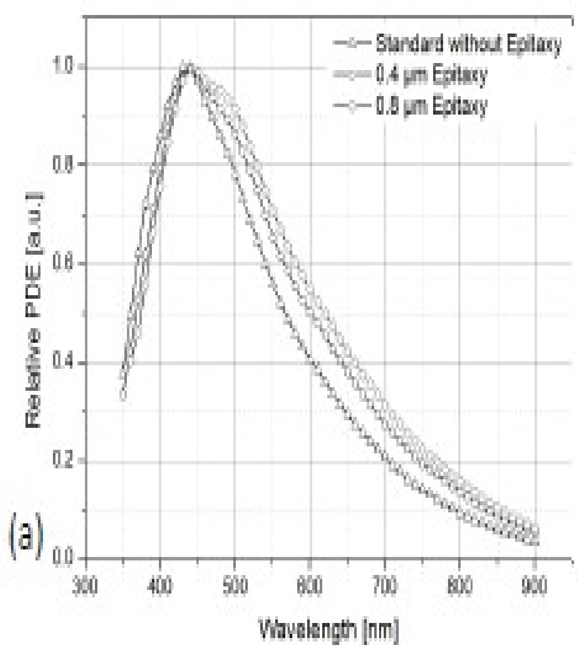

3)

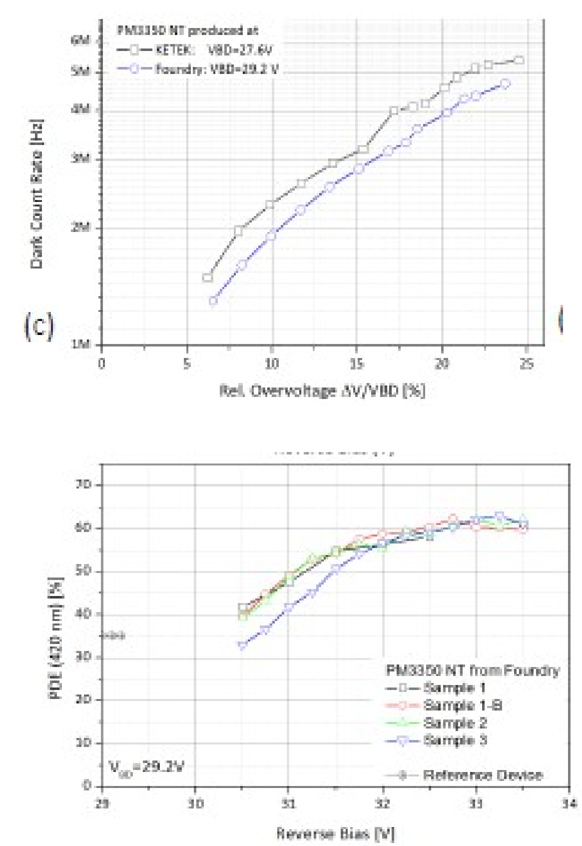

Poster ID 28 – John Murphy (Sens-L Tech. Ltd.) et al
Low Cost CMOS SiPM with Ultra-Fast Timing

Subject: recent news from SensL → new generation of p-on-n (custom process) devices
Features: 1) very low dark noise (100kHz/mm^2)
2) additional Fast Output → fast timing, sharp signal
3) good Vbreakdown and optical uniformity (sdev → few % level)

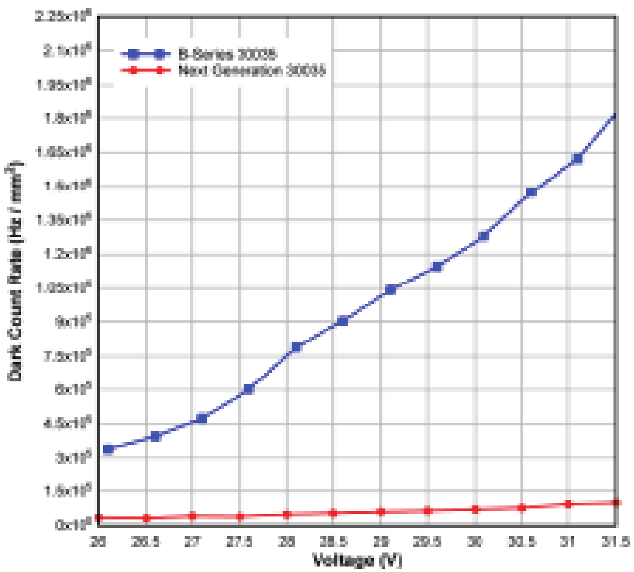

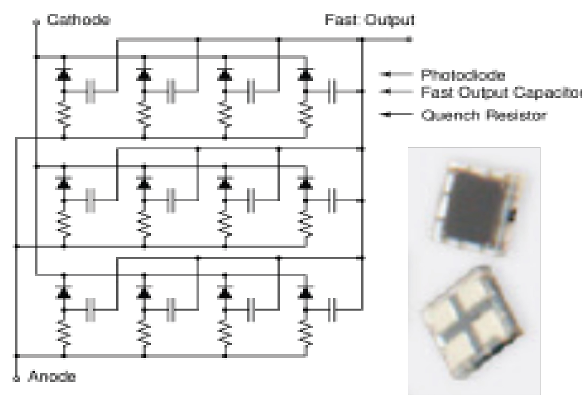

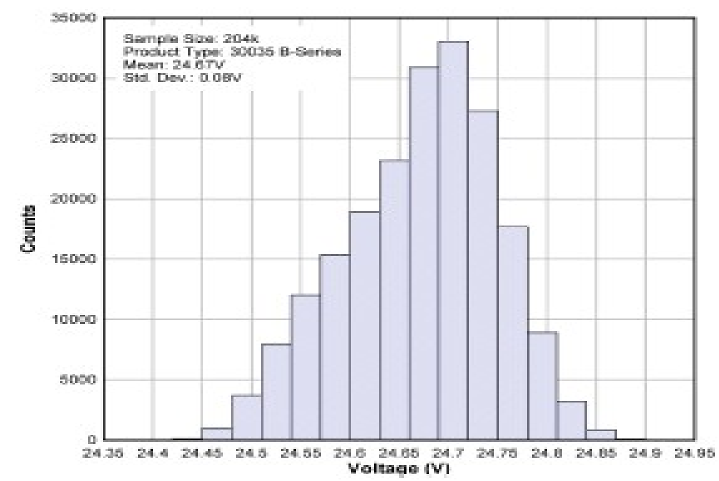

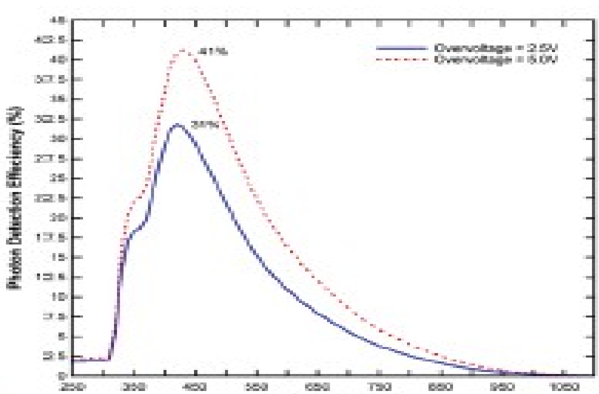

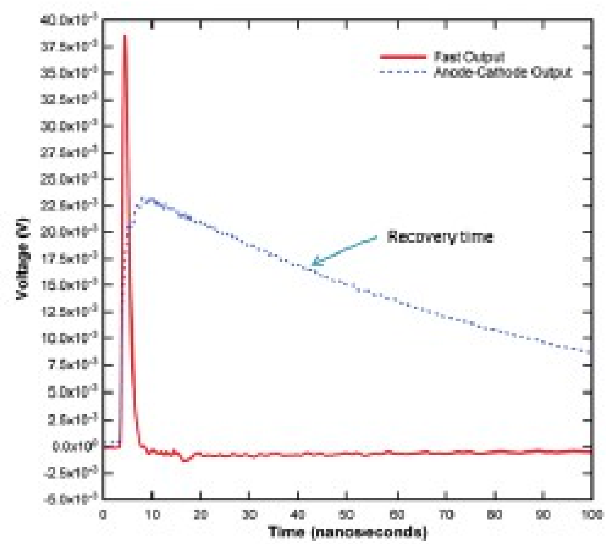

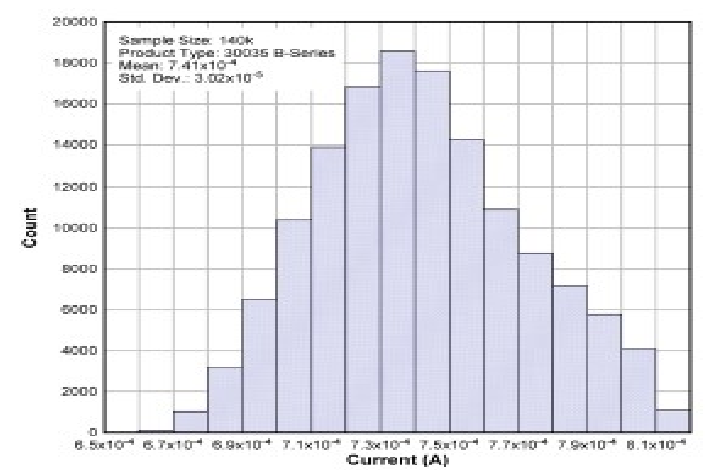

Poster ID 70 – Paola La Rocca (INFN, UniCa) et al

Fabrication, characterization and testing of silicon photomultipliers for the Muon Portal Project

Subject: large production by STMicroelectroncs → characterization of SiPM 2x2 array for use with scintillator bars + WLS fibers in Muon Tomography

Results: 1) batch O(10000) SiPM produced and encapsulated
2) standard functional static and dynamical tests
3) ~85% production yield

MUON 60 (test device of 1 mm^2)
PDE ~ 35 % (Δλ=500-550 nm, OV = 4V)
DCR ~ 500 kHz (0.5 pe, OV = 4V)
CROSS TALK = 0.46%

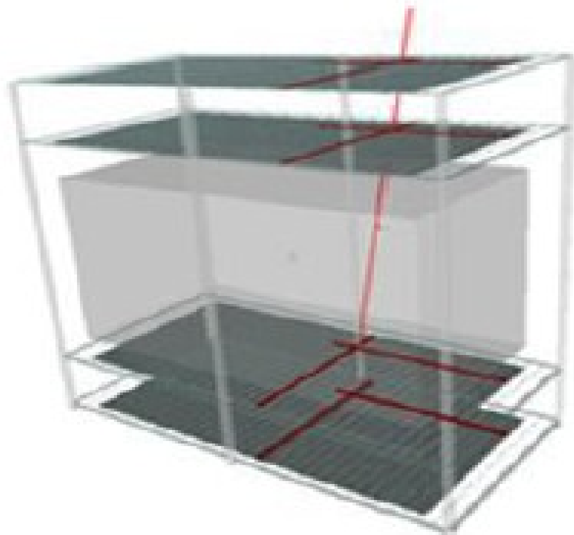

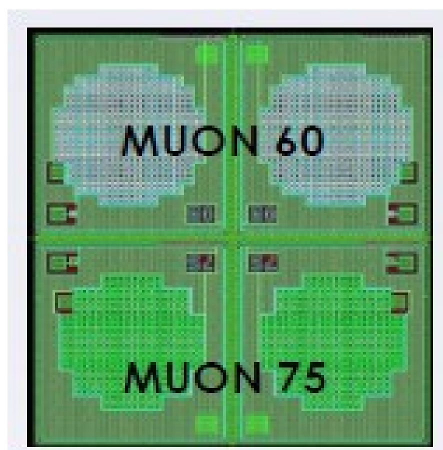

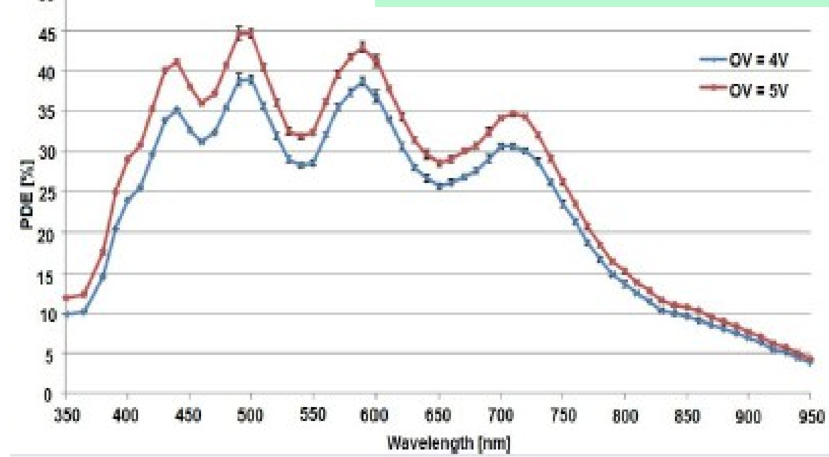

Silicon PhotoMultipliers custom-made by STMicroelectronics
- ✓ n-on-p technology
- ✓ 4 independent round shaped SiPMs (ϕ ~ 1.5 mm):
  - ✓ 2 MUON60 = SiPMs with 60 μm cell pitch
  - ✓ 2 MUON75 = SiPMs with 75 μm cell pitch
- ✓ Fill factor 67.4% (MUON60) and 73.8% (MUON75)

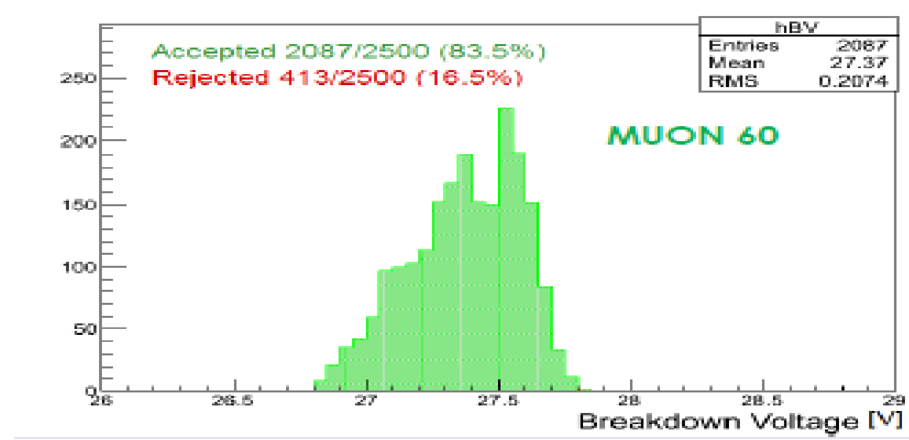

Hig

Poster ID 16 – Denis Pellion (CNRS Le2i) et al

Dark Count rate measurement in Geiger mode and simulation of a photodiode array, with CMOS 0.35 technology and transistor quenching

Subject: investigation about SPAD fabricated with AMS “CMOS-Opto” technology (0.35μm)

Results: 1) devices design and simulation: diffused guard ring and transistor quenching

2) chip realization → electrical characterization, Breakdown and Dark count measurement. Setup for PDE measurement

Design Layout → Realized chip → Packaging PGA68 → Read out circuit

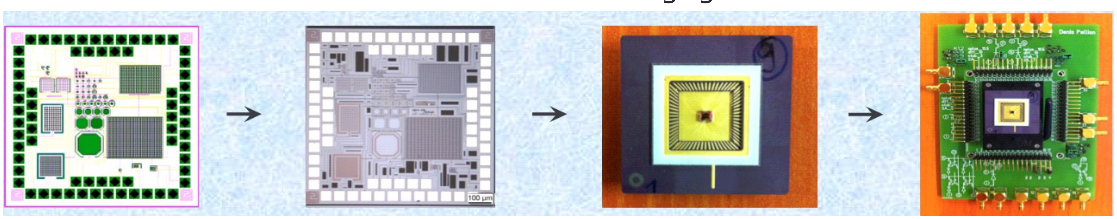

D (μm)	22.5°C Vbr (V)	22.5°C DCR at 800mV overvoltage (Count/s)	−40.0°C Vbr (V)	−40.0°C DCR at 800mV overvoltage (Count/s)
200	11.70	overflow	11.15	overflow
100	11.70	overflow	11.15	overflow
50	11.70	65000	11.15	45000
20	11.80	21000	11.18	1200
10	12.10	2020	11.49	270
7	12.90	1900	11.80	260
6	13.90	1900	12.40	260
5	16.20	1900	15.60	260

sion #1

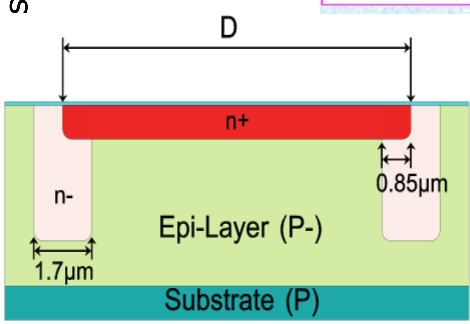

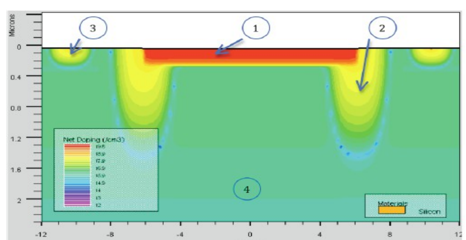

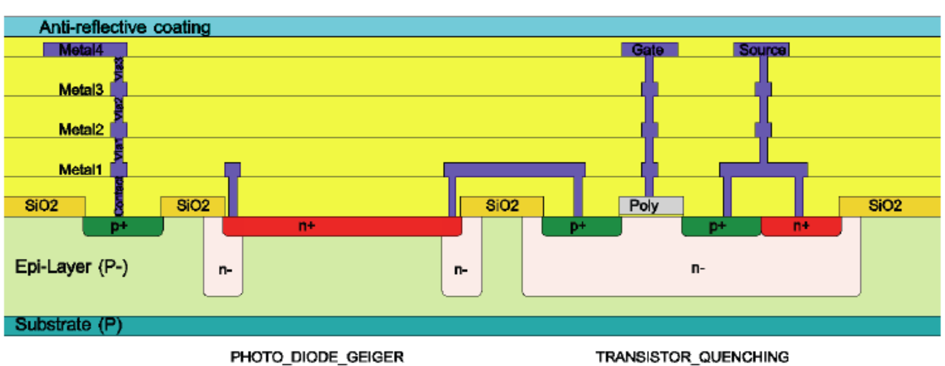

Figure 1: Cross-section of the Photodiodes design (SPAD) for Geiger mode in CMOS-Opto C35B401

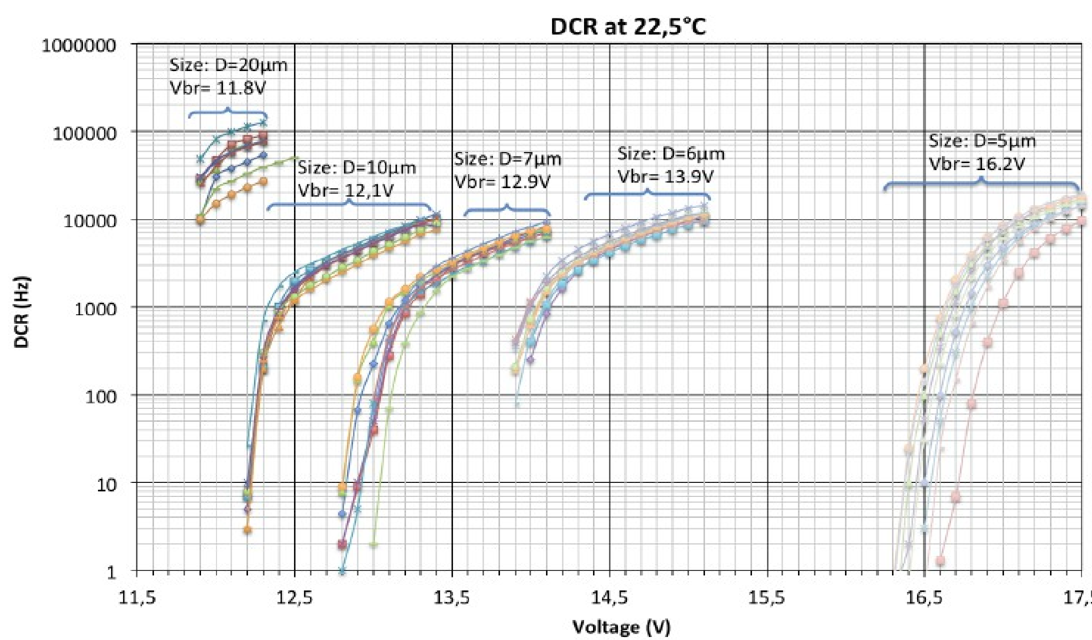

Figure 7: Dark count rate versus photodiode voltage at 22.5°C.

Poster ID 52 – Josef Blazej (Czech Tech Univ.) et al
Effective dark noise reduction by modified SPAD gating circuit

Subject: New operation scheme of SPAD with active gating and quenching

Results: Driving the excess voltage bias directly by the gate signal (instead of the output signal) results in effective reduction of after-pulsing noise. The shorter is the gate window, the more effective the scheme

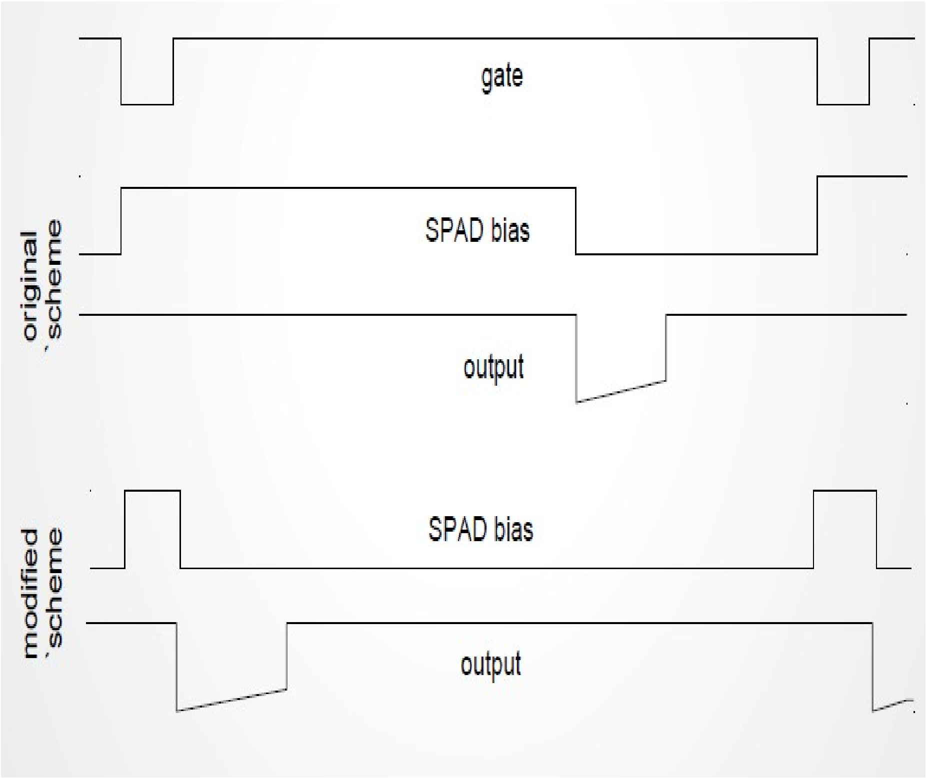

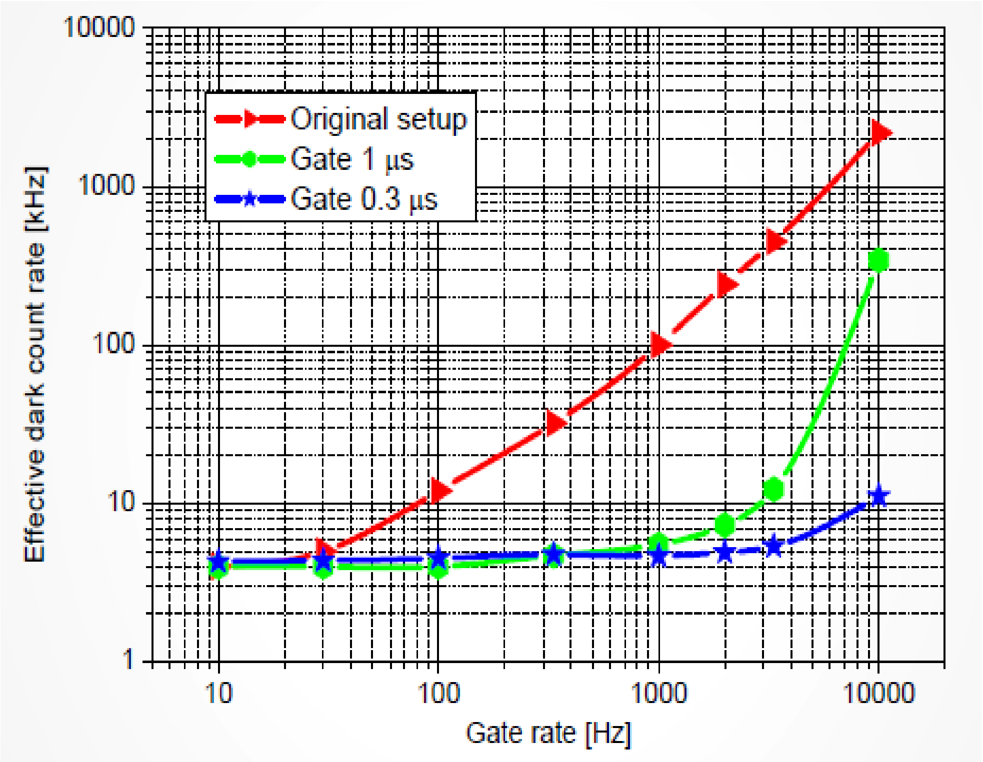

Poster ID 37 – Vladimir Zabrodskii (IPTI) et al

SiPM prototype efficiency for direct VUV registration

Subject: Spectral properties of SiPM prototype in vacuum ultraviolet region (VUV)

Results:
1) production of SiPM prototype → analog type, passive quenching, 10 pixels (p-on-n) diameter 100 µm, 50% fill factor
2) very interesting discussion about superficial region composition and structure and p-on-n vs n-on-p choice for VUV SiPM
3) Measured PDE ~ 4% in 112-180nm region

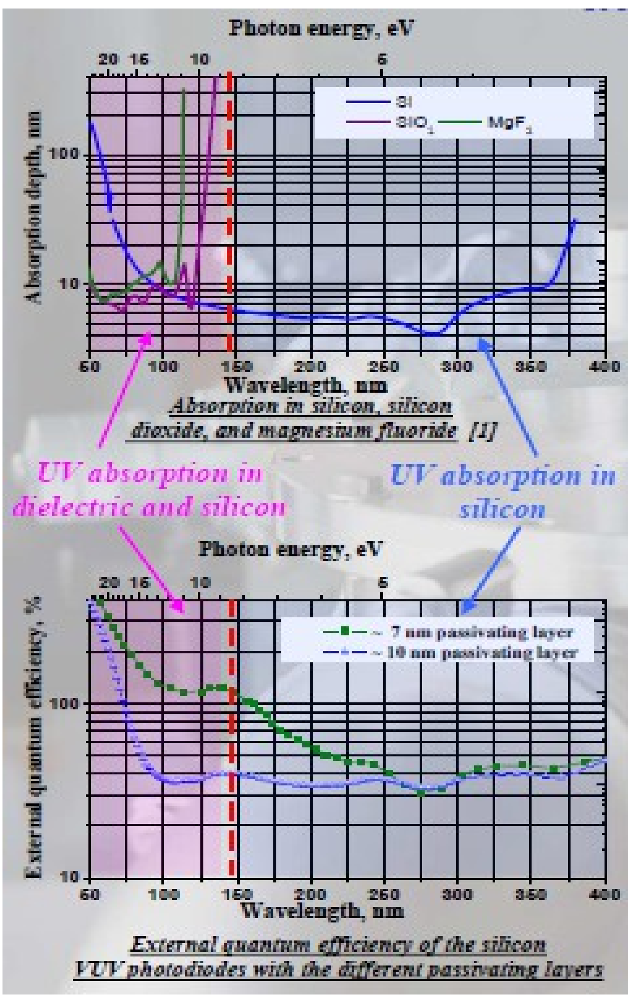

Absorption in silicon, silicon dioxide, and magnesium fluoride [1]

External quantum efficiency of the silicon VUV photodiodes with the different passivating layers

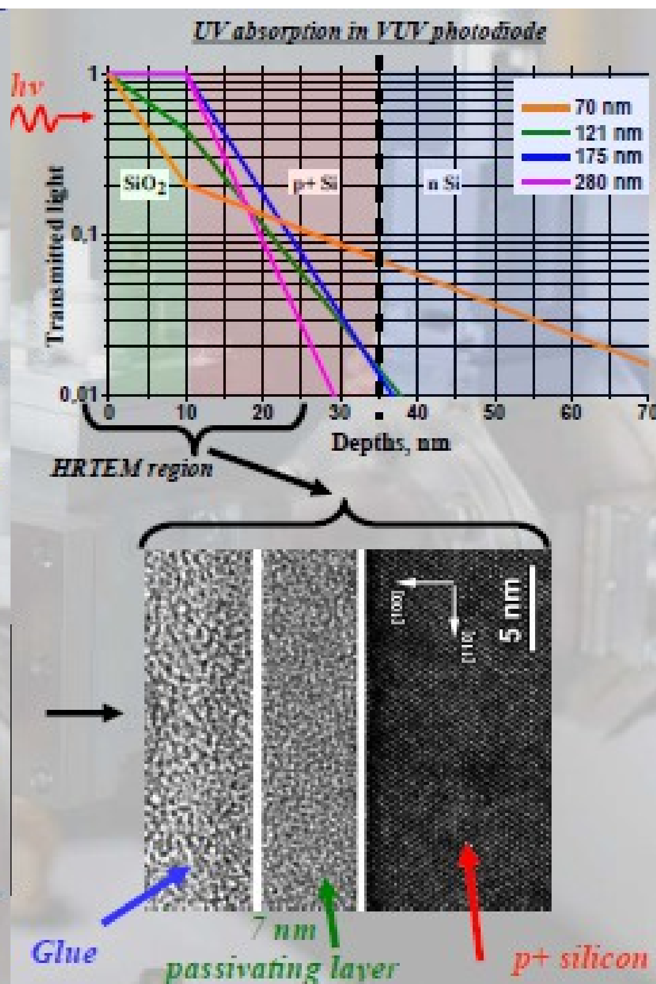

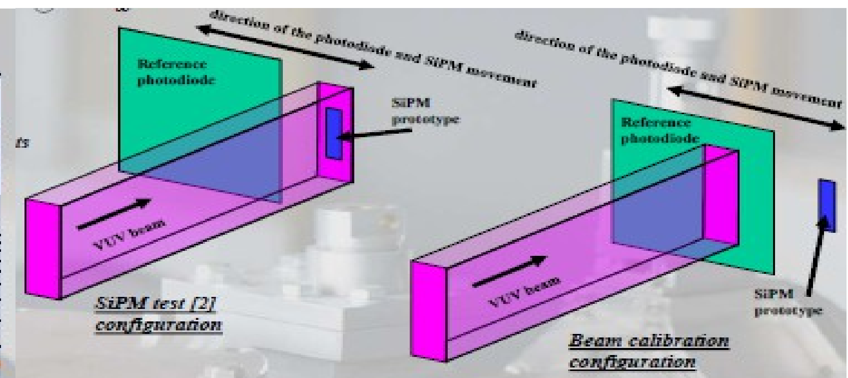

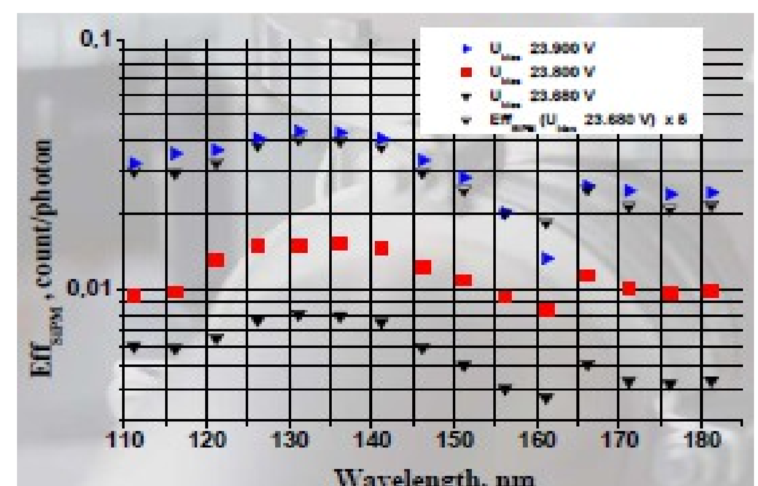

Poster ID 31 – Andrea Falcone (INFN and UniPv) et al

VUV and UV scintillation light detection by means of SiPM working at cryogenic temperature

Subject: characterization of SiPMs at cryogenic temperature and with VUV light

Samples: - AdvanSiD NUV-SiPM (optimized for UV, not for VUV region) and
- Hamamatsu VUV-MPPC (optimized for VUV region)

Results: Samples compared: AdvanSiD NUV-SiPM and Hamamatsu VUV-MPPC
1) breakdown voltage, quenching resistance, dark count rates, ...
2) PDE in VUV region (at room temperature)

SiPM	300 K	77 K	$\Delta V_{BD}/\Delta T$ given	$\Delta V_{BD}/\Delta T$ meas.
AdvanSiD	25.7 V	21.2 V	26 mV/°K	20 mV/°K
Hamamatsu	64.8 V	53.2 V	56 mV/°K	52 mV/°K

SiPM	300 K	77 K	$\Delta R_q/\Delta T$
AdvanSiD	2.6 MΩ	80 MΩ	347 kΩ/°K
Hamamatsu	321 kΩ	453 kΩ	600 Ω/°K

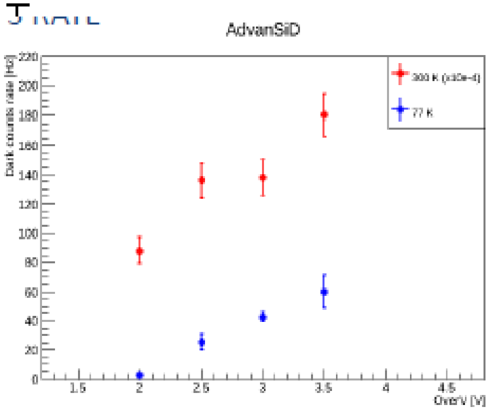

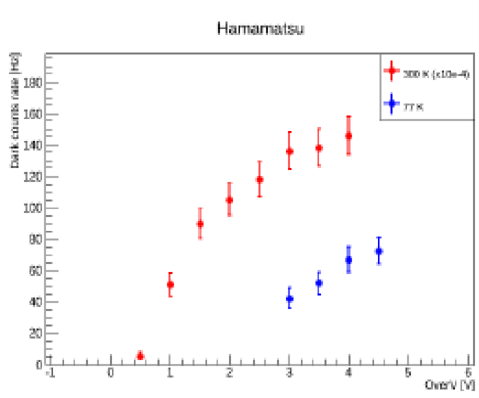

SiPM RESPONSE TO VUV

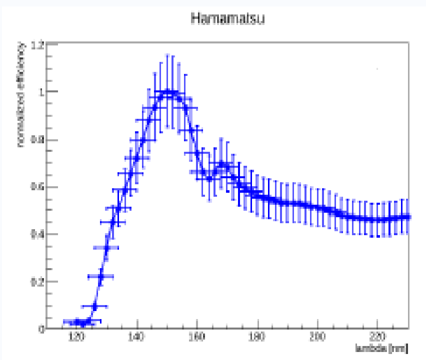

To understand the response of the SiPMs at VUV light, we perform a wavelength dependent analysis, ranging from 120 nm to 220 nm. The system is composed by:

- a Deuterium lamp;
- a VUV monochromator;
- a reference photodiode.

We show the ratio between the current produced in the reverse biased SiPM and in the reference photodiode. As expected, the two SiPMs are sensitive to different regions of the VUV spectrum.

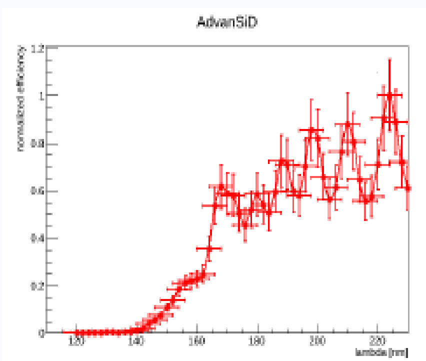

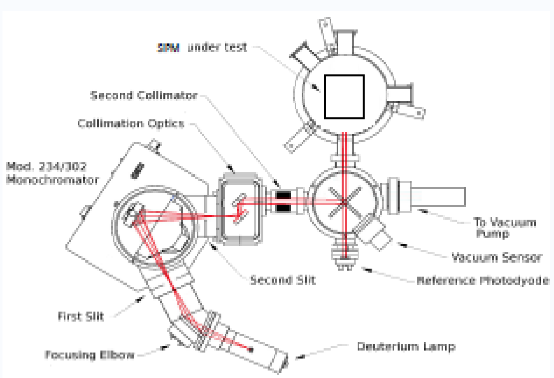

Poster ID 13 – Carsten Heidemann (RWTH Aachen) et al

Optical test set up for Silicon Photo Multipliers

Subject: Test station for temperature dependent complete characterization of SiPMs

Features:
- measurement of static and dynamics SiPM properties, noise (dark and correlated)
- temperature stabilization; range: -36°C → >60°C
- absolute PDE measurement both in CW and pulsed more; 250-1000 nm range

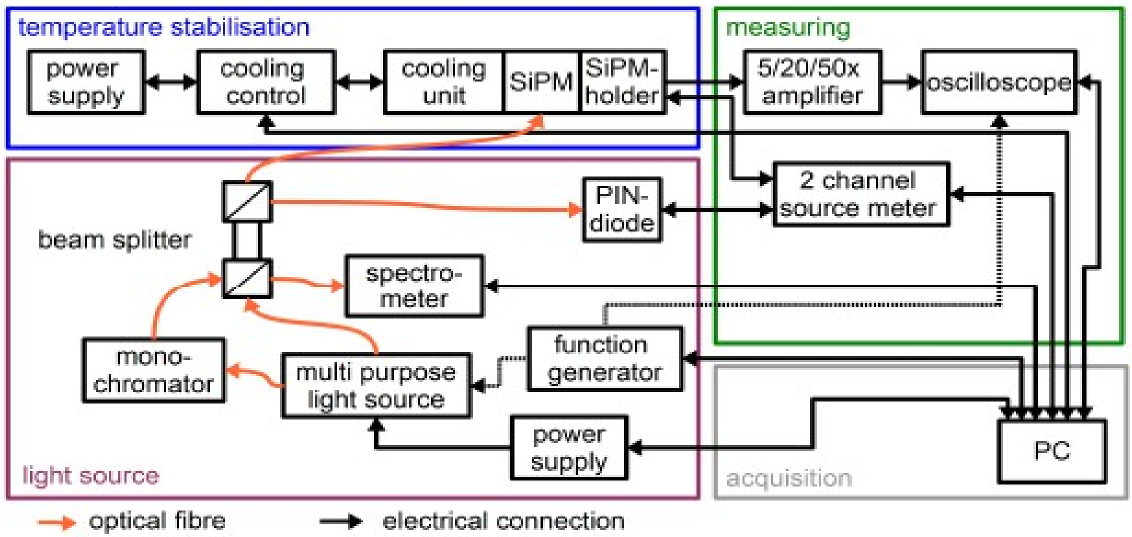

Reference detector

A calibrated PIN diode in combination with a source-meter is used to determine the light flux. The PIN diode is sensitive in the wavelength range from 250 nm to 1000 nm. In combination with the spectro-meter the absolute light flux can be determined.

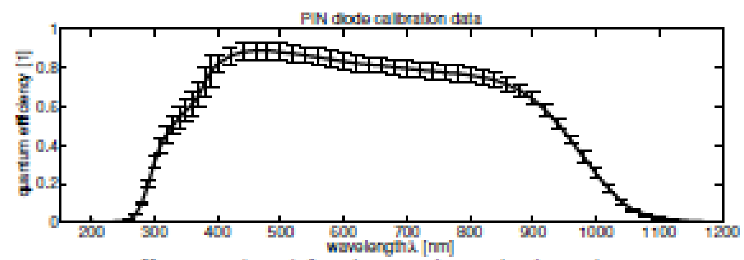

Quantum efficiency (q.e.) for the used PIN diode with 25mm² active area

Cooling and stabilization

The Peltier-based cooling unit allows to maintain a constant temperature from about -36 °C to greater 60°C. This allows to simulate the environmental condition for many experiments.

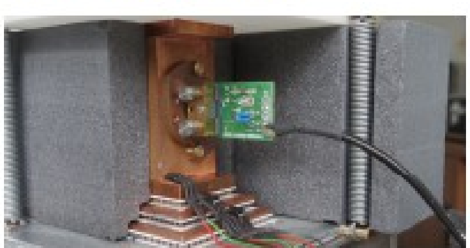

Cooling unit: 3 Peltier elements stacked on a large aluminum heat sink with forced airflow. Isolation partly opened for taking photo

Multi purpose light source

The LED-based light source offers DC and pulsed operation mode of LEDs with different wavelength in the spectral range from 315 nm to 700 nm.

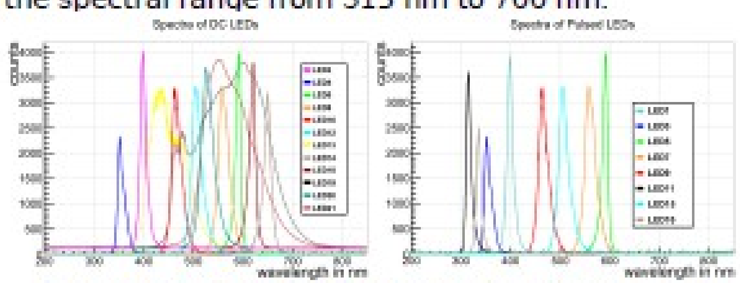

Spectra of the used LEDs for DC and pulsed operation mode

Poster ID 7 – Florian Scheuch (RWTH Aachen) et al
Electrical characterization and simulation of SiPMs

Subject: electrical model of SiPM and related parameter measurements
→ aim at best matching/design with front-end electronics

Results: 1) improved (* w/reactive elements) version of circuit based on "F.Corsi etal" model
2) measurement of relevant parameters (R, L, C) in wide frequency range and as a function of over-voltage
3) automatic procedure and temperature dependence foreseen

(*) high frequency behavior

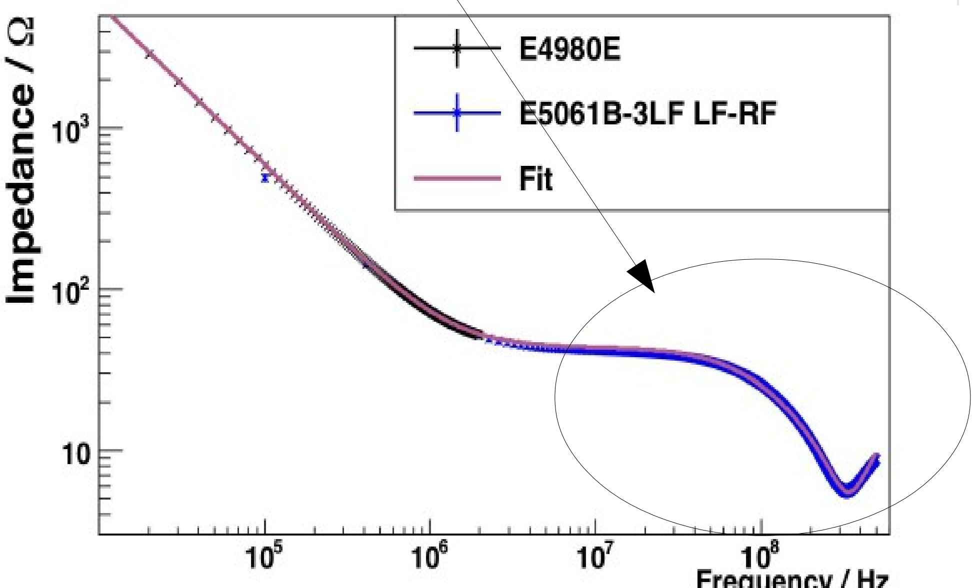

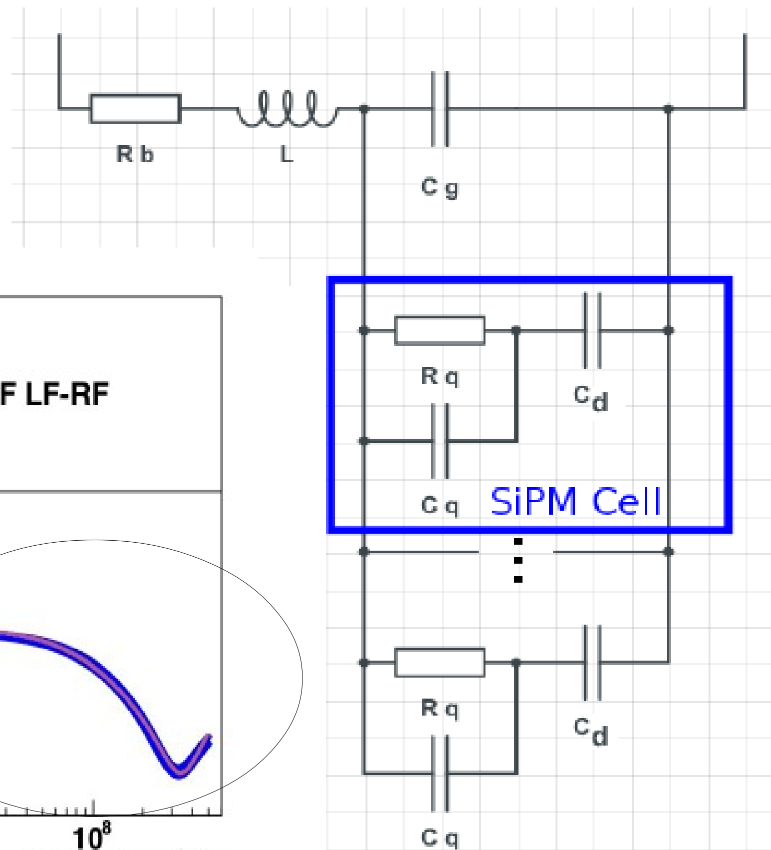

Poster ID 19 – Tim Niggemann (RWTH Aachen)
G4SiPM: a novel silicon photomultiplier simulation package for Geant4

Subject: parametric simulation of SiPM response → plug-in GEANT4

Results: 1) signal and noise (correlated and uncorrelated) are generated on a single cell basis accounting for the whole chain: including light source effects, entrance optics, photo-conversion, gain, recovery time and readout electronics effects
2) simulation validated by comparison with measurement of device response as a function of impinging photons (dynamic range)

Publicly available: forge.physik.rwth-aachen.de/projects/g4sipm

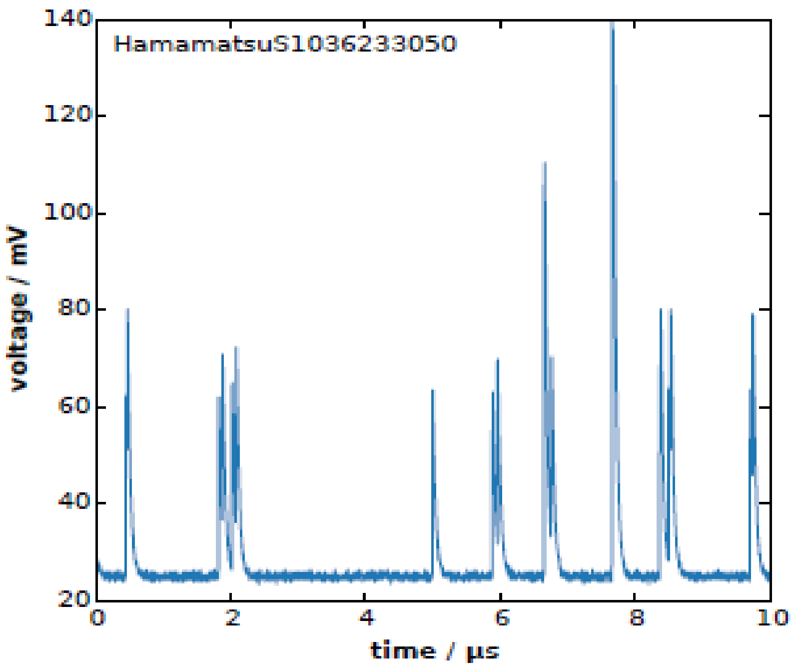

Simulated dark noise signal

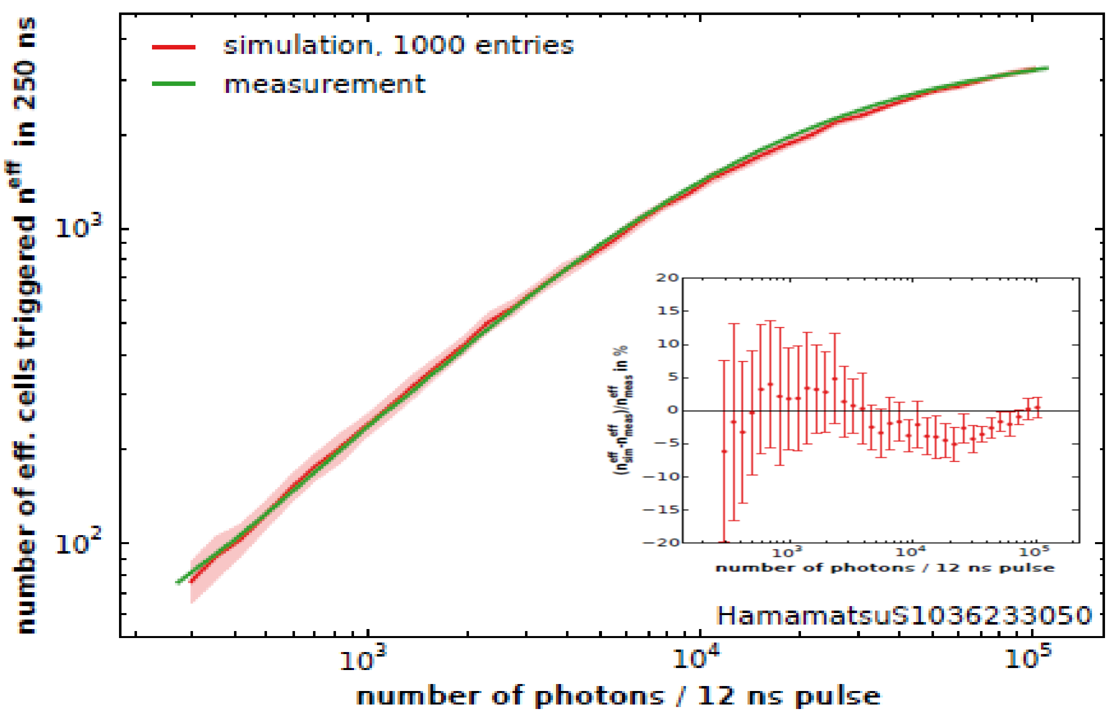

Poster ID 43 – Sergey Vinogradov (UoL) et al

The effect of SiPM dynamics on performance of fast X-ray detectors in cargo inspection systems

Subject: Studies of SiPM response for reading out continuous modulated light signals with applications in X-rays cargo inspections or beam loss monitors

Results: Study of response dynamic evolution in time (waveform shape):

1) pulsed mode → binomial distribution works well
2) continuous light, constant intensity → non-paralizable dead time (exponential recovery)
3) continuous but amplitude modulated light (CML) → in between !

→ first approximation model for current waveform shape

Note: recovery time and after-pulsing → high frequency cutoff in CML response

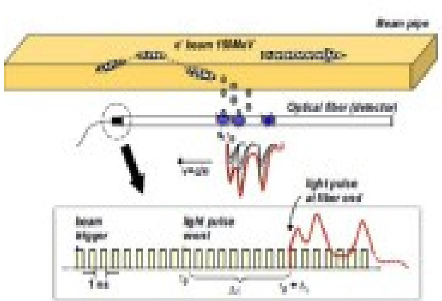

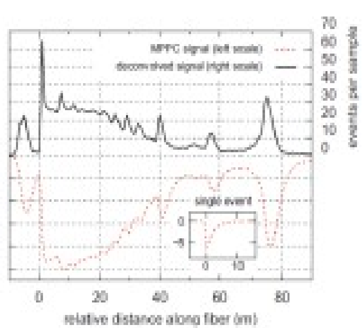

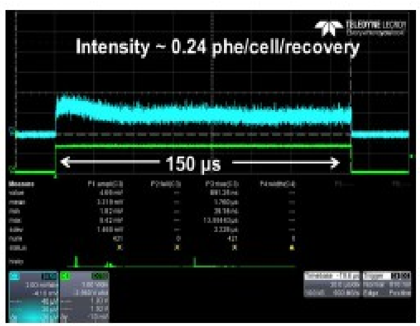

Low light intensity, ~ linear response

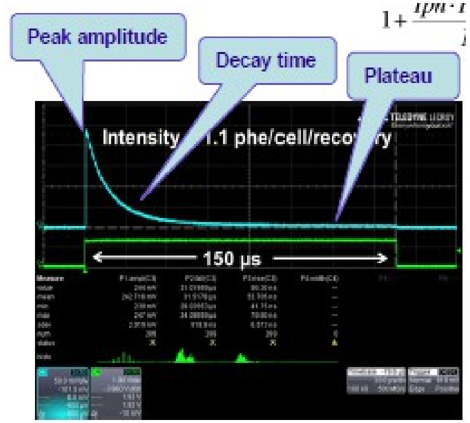

Mid light intensity, non-linear response

High light intensity, high overload

$$Nfired(t) = Ncell \cdot \exp\left(-\frac{Nph(t)\cdot PDE}{Ncell}\right)$$

Tpulse < Trec binomial distribution

$$Nfired(t) = \frac{Nph(t)\cdot PDE}{1+\frac{Nph(t)\cdot PDE\cdot Trec}{Ncell\cdot Tpulse}}$$

Tpulse > Trec non – paralizible dead time

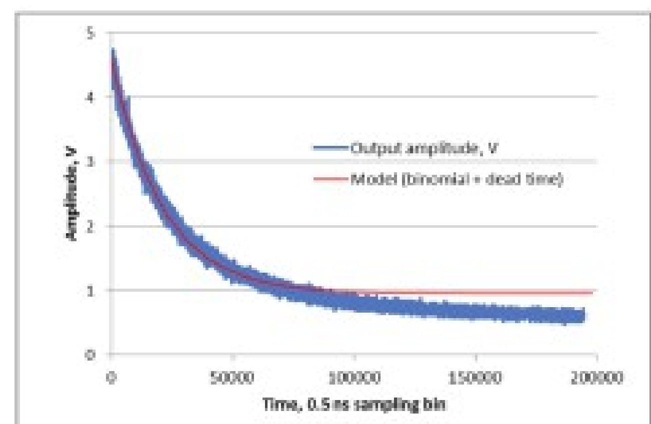

Devices and properties of SiPM/SPAD

Devices and characterization
- SiPM devices/ new features
- VUV sensitivity and cryogenic characterization
- Characterization vs models / simulations

Timing properties
- intrinsic timing
- timing performances in applications

Systems – Applications using SiPM

Cherenkov (RICH, Cherenkov Telescope camera)
Scintillators (crystals, neutron det., plastics)

Other Photo-detectors / Systems

Poster ID 46 – Fabio Acerbi (FBK) et al
High single-photon time resolution SiPM

Subject: very accurate experimental study of SiPM intrinsic timing fluctuations:
mainly dependence on device size by from single SPAD to SiPM

Results: 1) main contribution at device level → device capacitance
(signal propagation: second order effect; device uniformity: negligible contrib.)
2) main contribution at single cell level → lower field at cell edges
(with single cell, single photon resolution below 20ps "easily" reached)

Single-photon time resolution (FWHM) at λ = *425 nm*

- for the 1x1 mm² SiPM: **80 ps** at 7.4 V
- for the 3x3 mm² SiPM: **180 ps** at 6 V
- for 1-single 50µm cell: **55 ps** at 8 V

Single-photon time resolution (FWHM) at λ = *850 nm*

- for the 1x1 mm² SiPM: 115 ps at 7.5 V

Causes of SPTR worsening increasing the dimension of device?

1. Measurement with pinhole
   - *good uniformity*
   - this is not the limiting factor
2. Rising-edge slope decreases for bigger devices (higher capacitance)
   - first-approximation analysis indicates *this is an important factor.*

SPTR of circular SPADs
→ analysis of structural limiting factors

1. Metal ring all-around active area
   - Better signal extraction
2. Covering of the edge of active area
   - Better time resolution
   - FWHM ~ 20ps

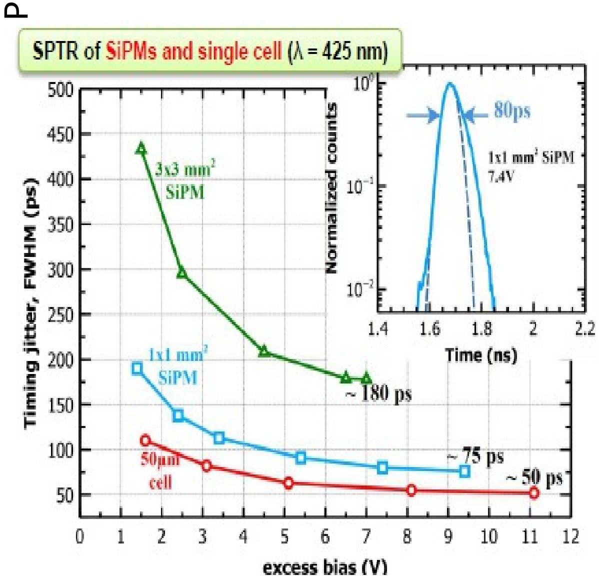

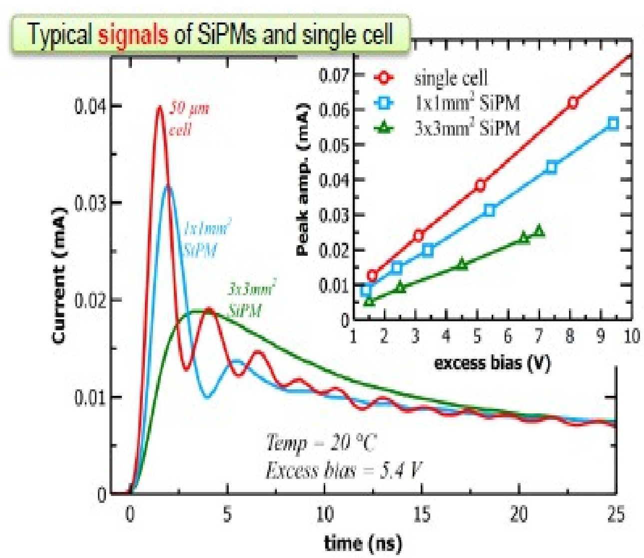

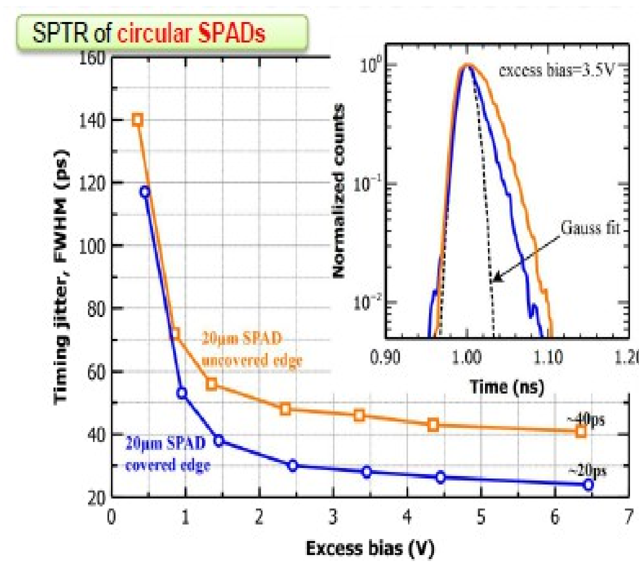

Poster ID 4 – Elena Popova (MEPHI) et al
Amplitude and Timing properties of a Geiger discharge in a SiPM cell

Subject: avalanche discharge properties of a single SiPM cell (SPAD) as function of number of impinging photons (photo-electrons): by comparison measured waveform vs avalanche propagation model

Results:
1) more ph.e → earlier avalanche and smaller jitter
2) same developed charge → higher and sharper waveform peak
3) timing jitter limited by avalanche lateral spread

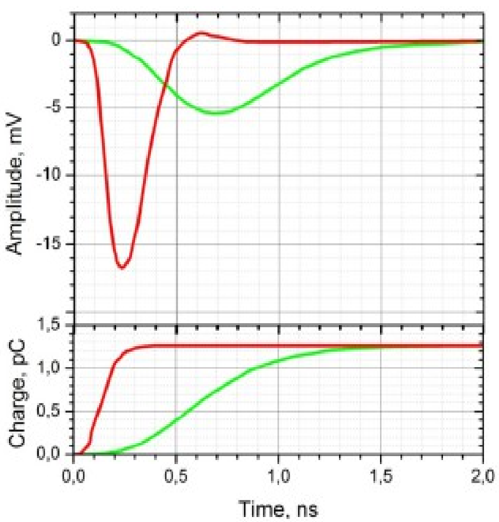

SPICE simulated pulses and total charge for one SiPM cell in case of single phe (green curves) and 100 phe (red curves)initial spots

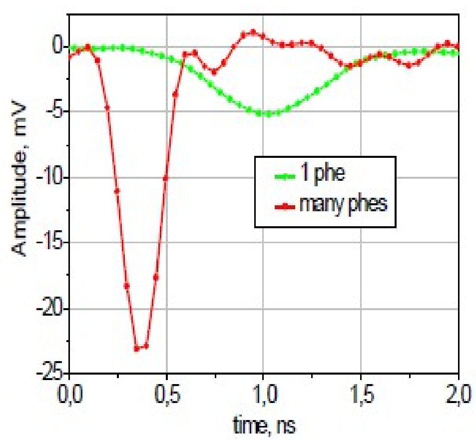

Scope pulses for one SiPM cell in case of single phe (green curves) and many phe (red curves) initial spots

SPTR for single standalone SiPM cell

Digital scope **LeCroy WaveRunner 620Zi 2GHz**
FEMTO-T laser system with 176 fs FWHM, and λ=876nm
focused to **2 μm** at the center of a stand-alone SiPM cell

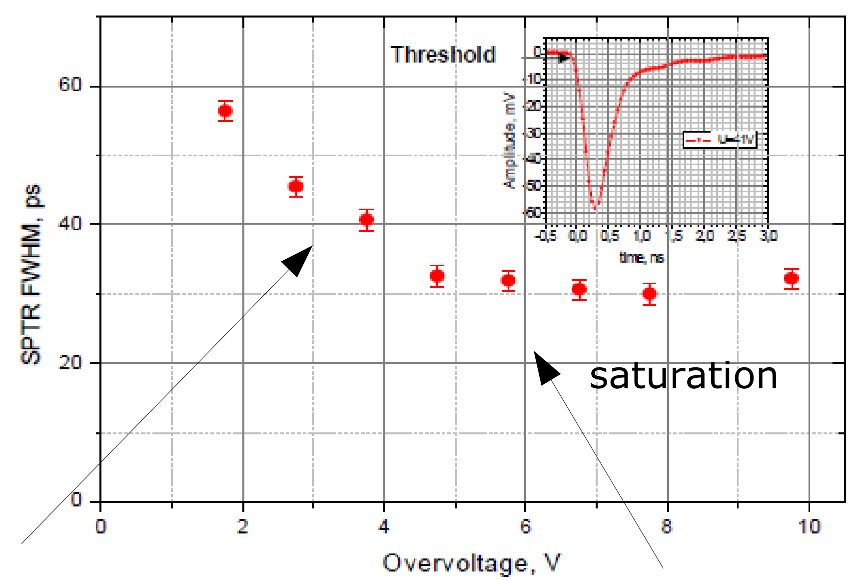

main contribution longitudinal avalanche development

main contribution lateral spread

Poster ID 22 – Sergei Dolinsky (GE Global RC) et al

Timing resolution performance comparison of different SiPMs

Subject: factors limiting time resolution of system SiPM+LYSO crystals for TOF-PET

Results: Main contributions to system time resolution

1) Single photo electron (SPE) pulse shape:
extent of falling tail (R quenching) → rise time of scintillator pulse
2) variance of signal propagation time from cell to anode/cathode
3) crystal longitudinal dimension

Anyway: the various SiPM samples behave differently concerning pulse shape and dark rate, yet, working at same PDE → yield similar coincidence resolving time (CRT)

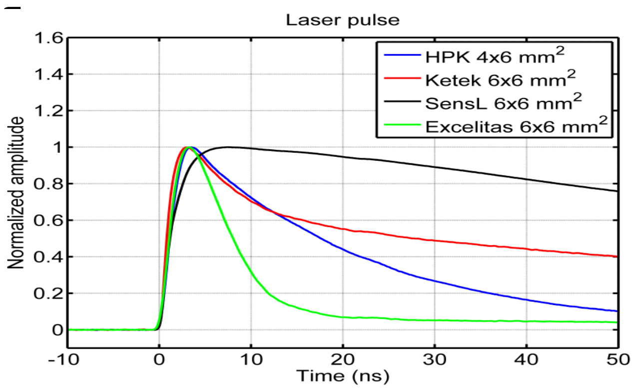

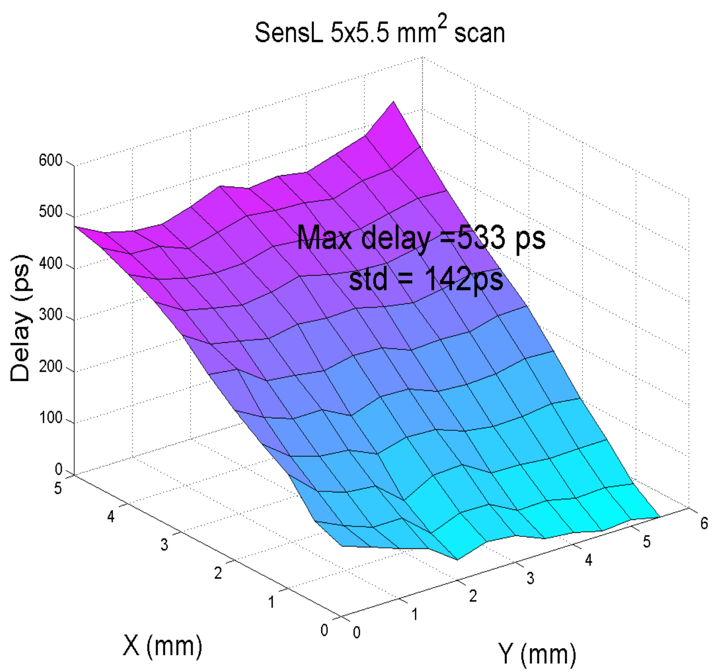

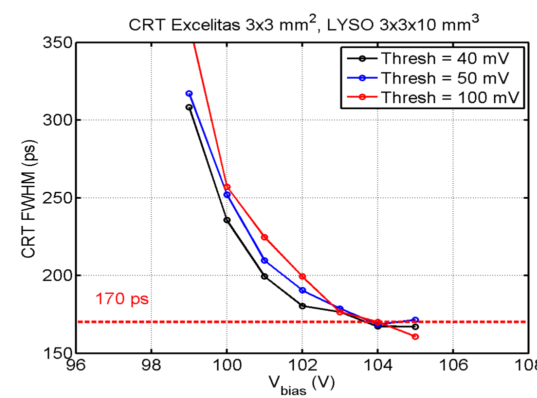

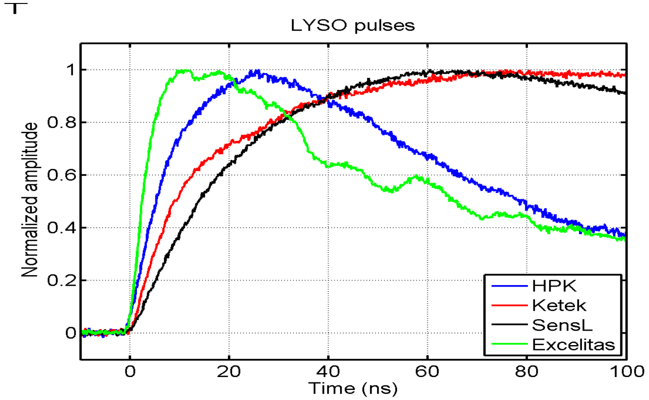

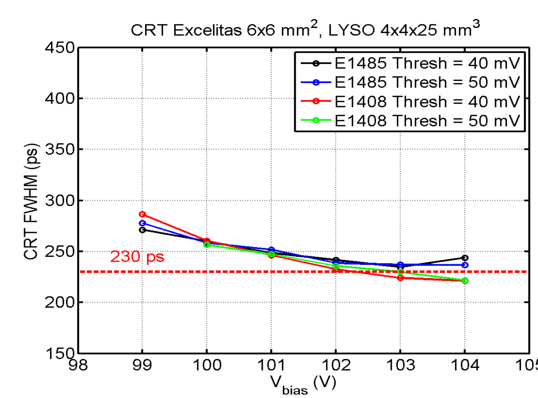

Poster ID 1 – Stefan Gundacker (CERN) et al

On the comparison of analog and digital SiPM readout in terms of expected timing performance

Subject: simulation of systems composed by digital or analog SiPM + LSO for TOF-PET
→ comparison of timing performances w/ 511keV gammas

Note: analog SiPM w/ threshold discrimination → only 1 possible type of combination of photons times (estimator of scintillation event time) → average time
digital SiPM provides all photons times of arrival → various possible "machine time"
→ two estimators tested: average time and max. likelihood time

Results: 1) simulation of system analog SiPM validated by comparison w/ CRT data
2) comparison of simulation: same best timing performances for analog and digital but digital allows higher threshold
NOTE: after-pulses and Xtalk not yet included in digital SiPM simulation

MC Validation (analog SiPM)

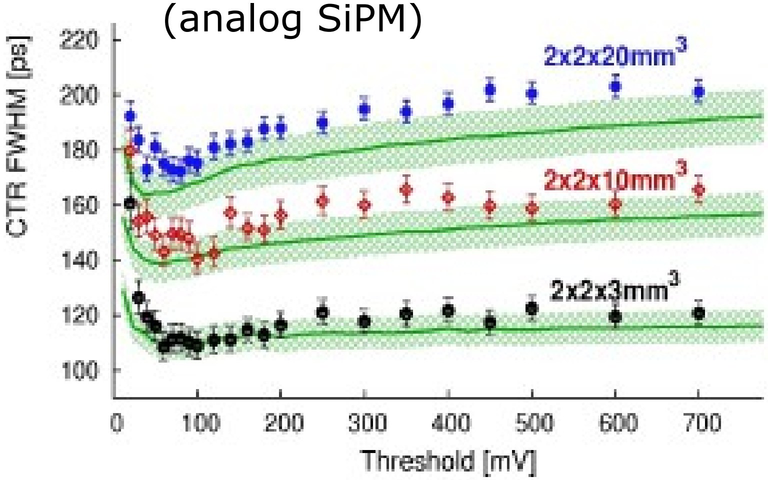

Simulations accurately accounts for different crystal lengths

MC comparison

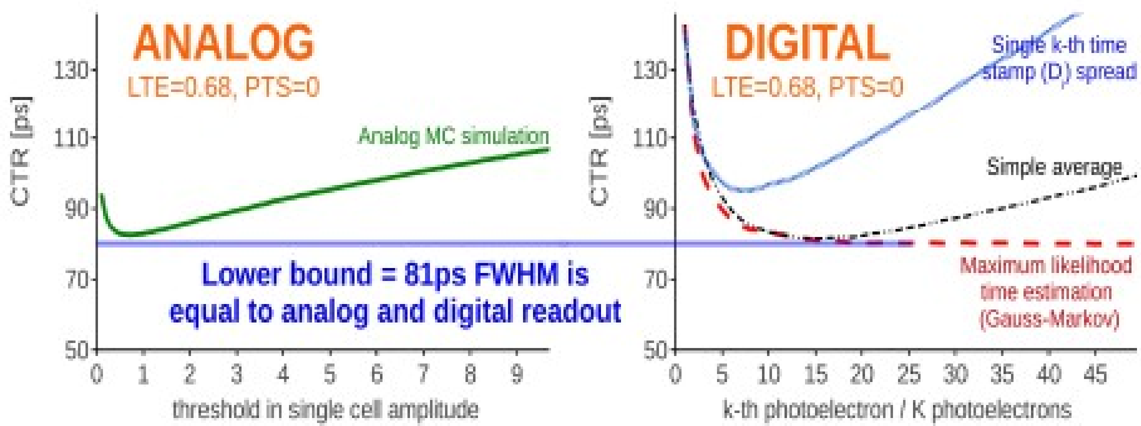

Devices and properties of SiPM/SPAD

Devices and characterization
- SiPM devices/ new features
- VUV sensitivity and cryogenic characterization
- Characterization vs models / simulations

Timing properties
- intrinsic timing
- timing performances in applications

Systems – Applications using SiPM

Cherenkov (RICH, Cherenkov Telescope camera)
Scintillators (crystals, neutron det., plastics)

Other Photo-detectors / Systems

Poster ID 34 – Elvedin Tahirovic (JSI) et al
Characterization of the Hamamatsu MPPC S11834 as a Photon Sensor for RICH

Subject: test of a system made by matrix 8x8 SiPM matrix (Hamamatsu) + quartz light concentrator (matrix of cones) for proximity focusing RICH light readout system

Results: laser scan and test beam with electrons 5GeV across aerogel

1) Excellent light readout with SiPM also for Cherenkov detector (low light appl.):
→ high PDE and dark noise mitigated by light concentrator and time coincidence

2) SiPM-concentrator optical coupling is critical: Cherenkov light is polarized

Highlights Poster Session #1

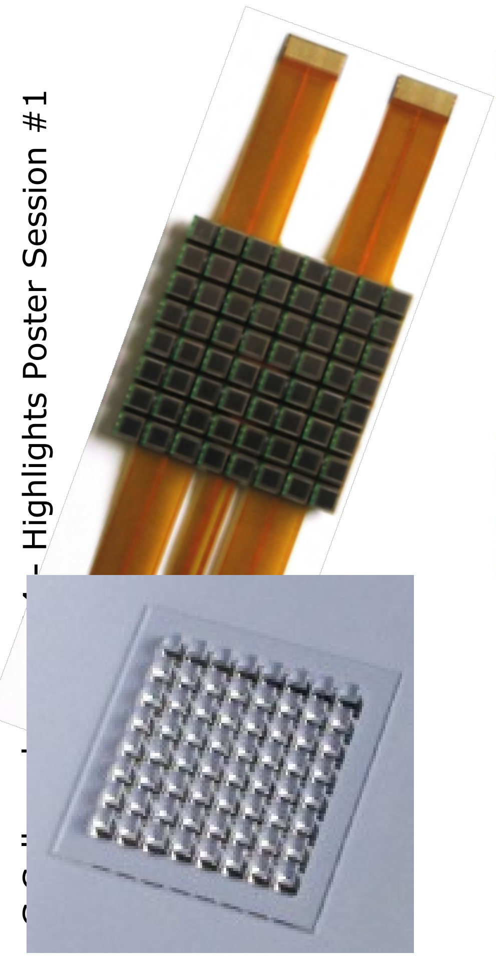

Response to low intensity light

Response of the module to attenuated picosecond laser pulses in narrow time detection window (10 ns)

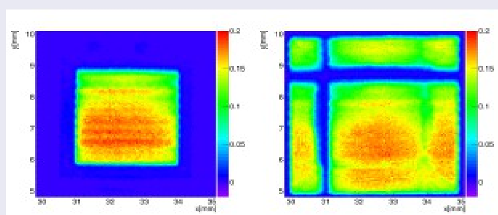

Scan without (left) and with light concentrators on (right). Laser beam was focused to $\sigma = 50\mu$m. The observed number of photons is 2.1 times higher in latter case. The empty bands are due to misalignment

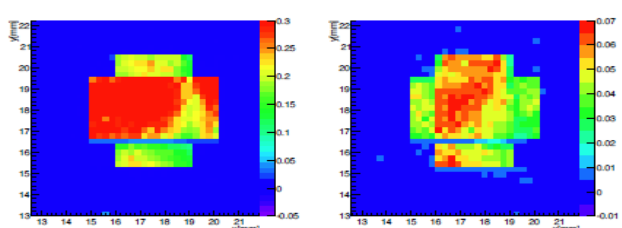

Fig. 4. The response of the MPPC to linearly polarized light. The polarization axis on the two histograms differs by 90 degrees.

Detected photons with light concentrators

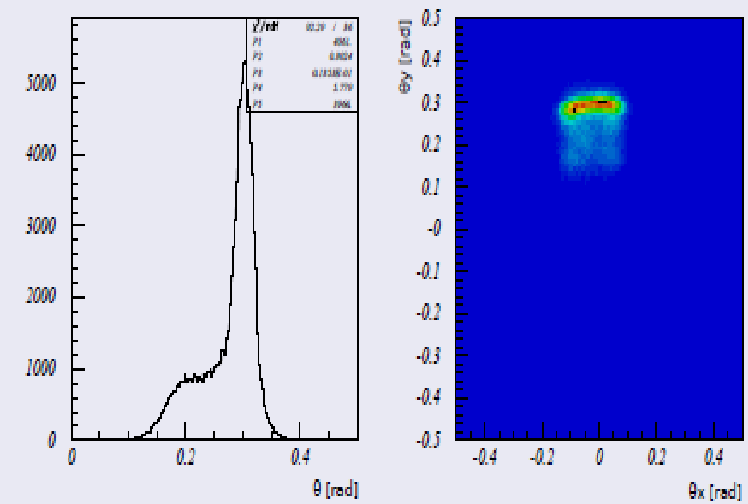

Hits distribution with respect to corresponding Cherenkov angle (left). Accumulated hits in Cherenkov angle space (right). Only 1/9 of the ring circumference was covered by one module.

Poster ID 49 – Matthieu Heller (DPNC UniGe) et al

Characterization of large area SiPM for gamma-ray astronomy

Subject: new large area SiPM for use in Cherenkov telescope camera

Results: 1) coupling w/ hollow hexagonal light concentrator w/ high efficiency (~90%)

2) development w/ Hamamatsu of hexagonal large area (~95mm^2) SiPM (4 ch.)

→ full characterization (static/dynamic, charge resolution, noise, PDE,...)

3) Transimpedance Op Amp readout 2 channels in parallel

→ analog sum of 4 channels → sampling 12bit@250MS/s

Main issue: large total capacitance O(800pF)

→ sensor response does not agree w/ electrical models

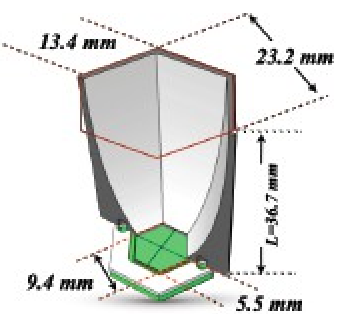

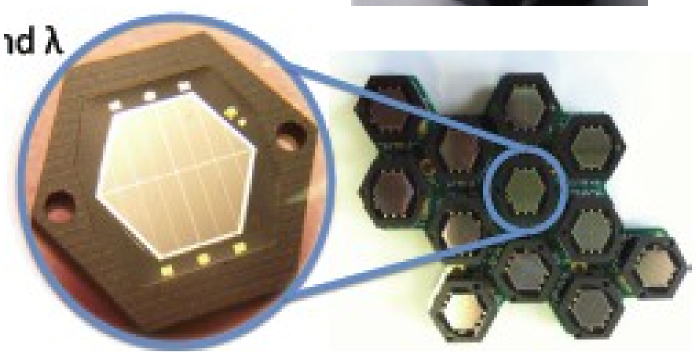

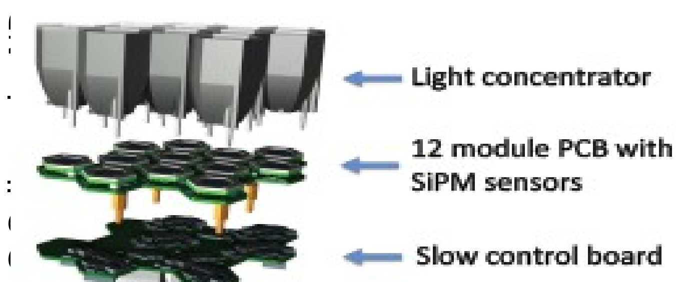

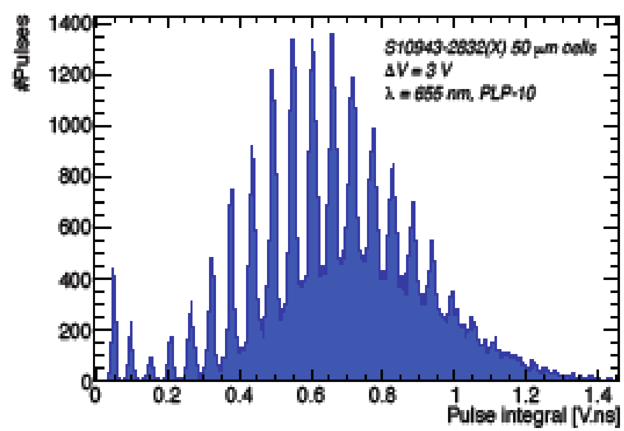

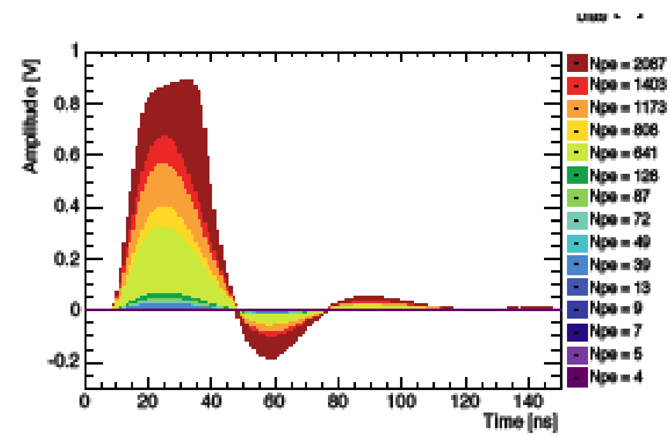

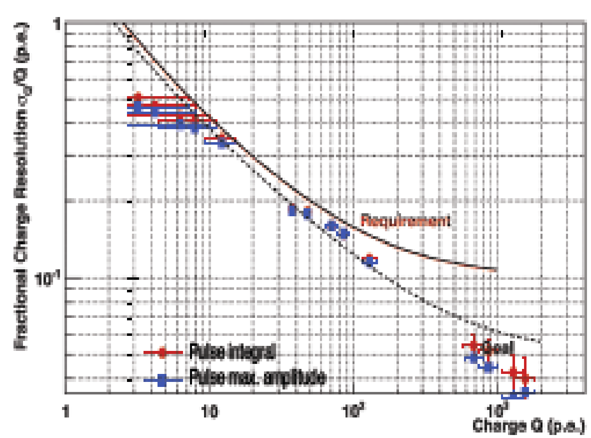

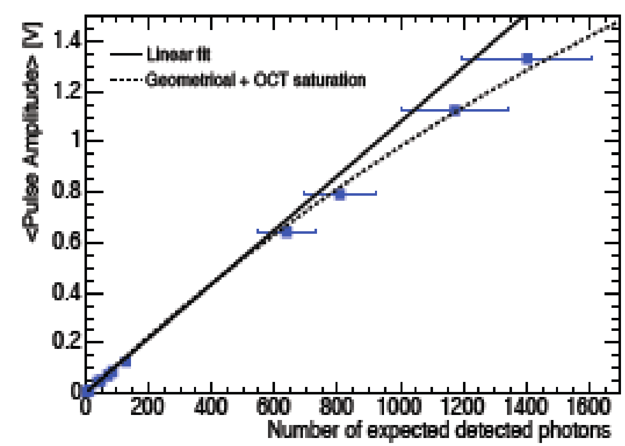

Poster ID 61 – Amadeo Iborra (I3M Valencia) et al
Detector block based on arrays of 144 SiPMs and monolithic scintillators: a performance study

Subject: on-line reconstruction of impact position of γ-ray on monolithic LYSO crystal.
Scintillation light readout by SiPM matrix ($5x5cm^2$ active area /12x12 channels)
Analog SiPM readout by 3 ASICs performing CoG and DOI reconstruction

Results: trapezoidal crystal shape for reducing edge effects
1) wrapping by teflon or Enhanced Specular Reflector → best energy and time res.
2) black painting on 5 sides → best position resolution w/ few 20% worse energy

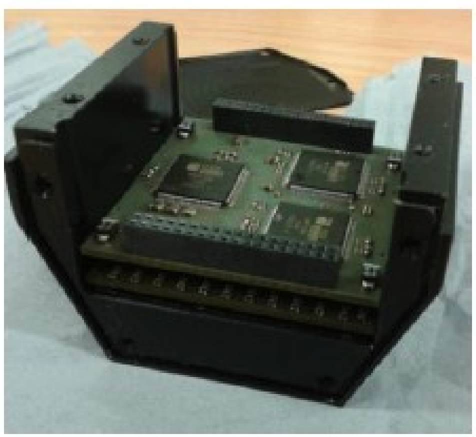

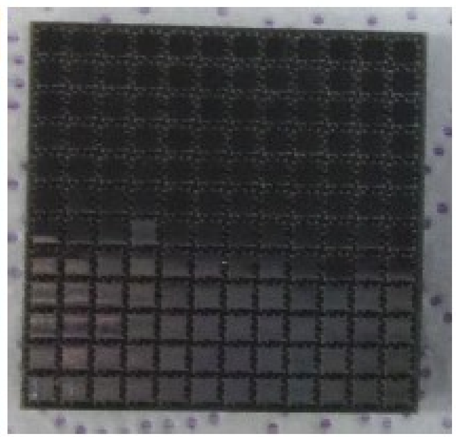

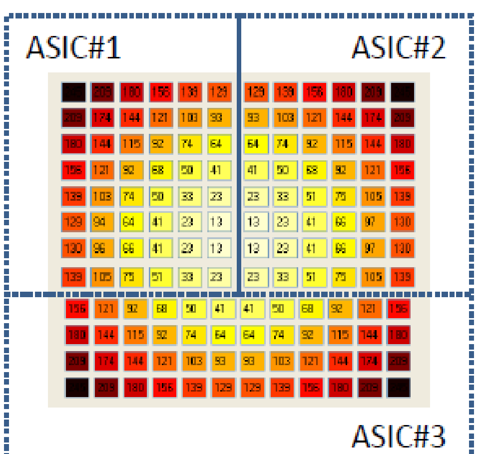

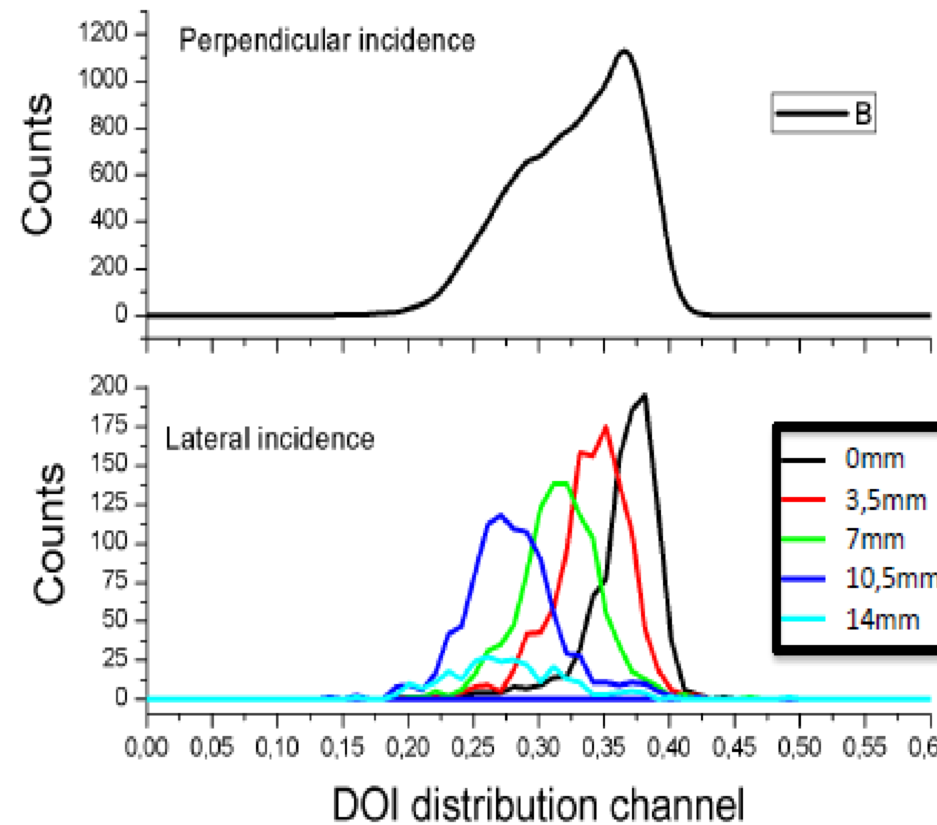

Poster ID 25 – Pablo Conde (I3M Valencia) et al
Neural network positioning algorithm with dSiPMs and monolithic crystals

Subject: off-line reconstruction of impact position of γ-ray on monolithic LYSO crystal. Scintillation light readout by digital SiPM (3.26x3.26 cm^2 active area /64 channels)

Results: Need black painting on 5 crystal sides; need peltier cooling of digital SiPM
1) measurements demonstrate that Neural Network reconstruction doesn't suffer compression → overperforming classical moments (CoG) method
2) accurate NN training is critical

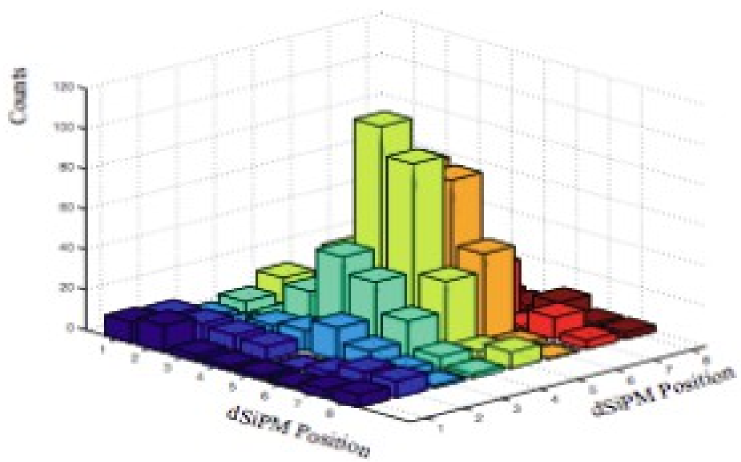

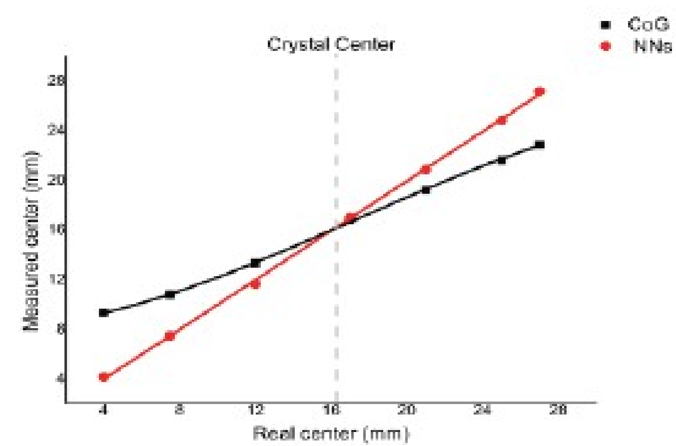

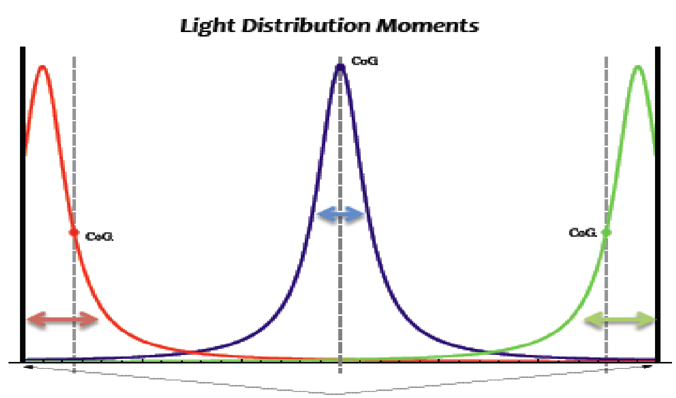

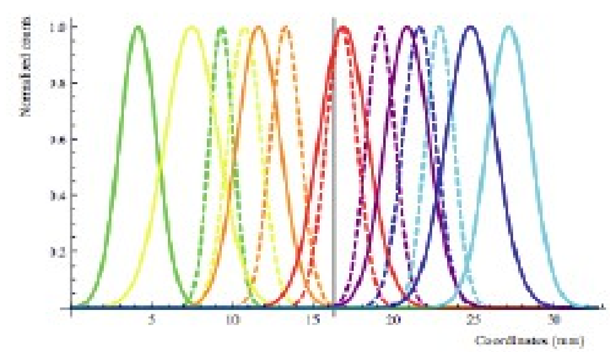

G.Collazuol - NDIP14 - Highlights Poster Session #1

Poster ID 73 – Massimo Caccia (UINS) et al

A fast neutron detector for homeland security based on scintillation light by a noble gas sensed by Silicon Photomultiplier arrays

Subject: fast neutron detector based on high pressure ^4He scintillation+WLS readout by SiPM

Results: 1) prototype detector

- based on ARKTIS tube concept: ^4He @180bar + reflector w/ WLS coating + windows + PMT → substituted by SiPM 4x4 matrices
- SiPM have no problems in He → inside the tube: no optical windows, more photons

2) very effective n/γ pulse shape discrimination (delayed coincidence scheme)

→ γ rejection ~ 10^6 with n detection efficiency ~3%

#1

ARKTIS tube

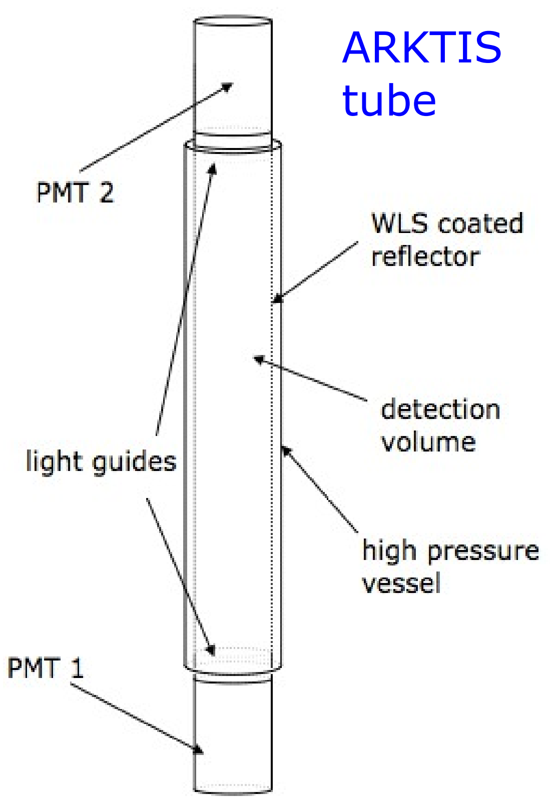

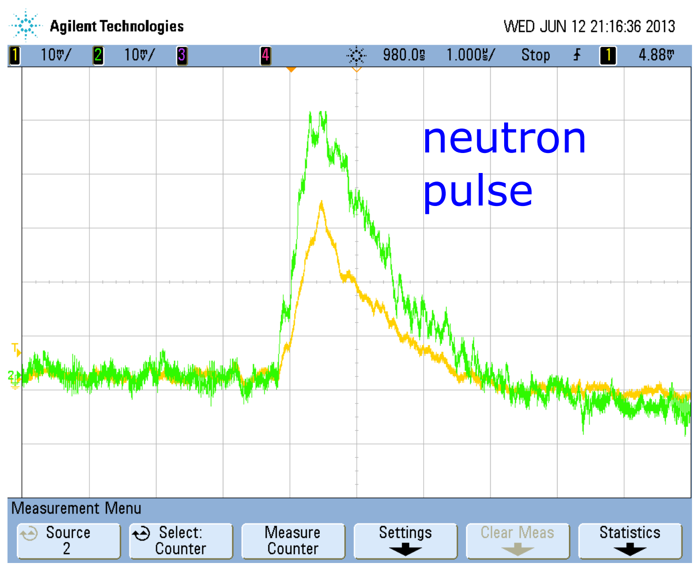

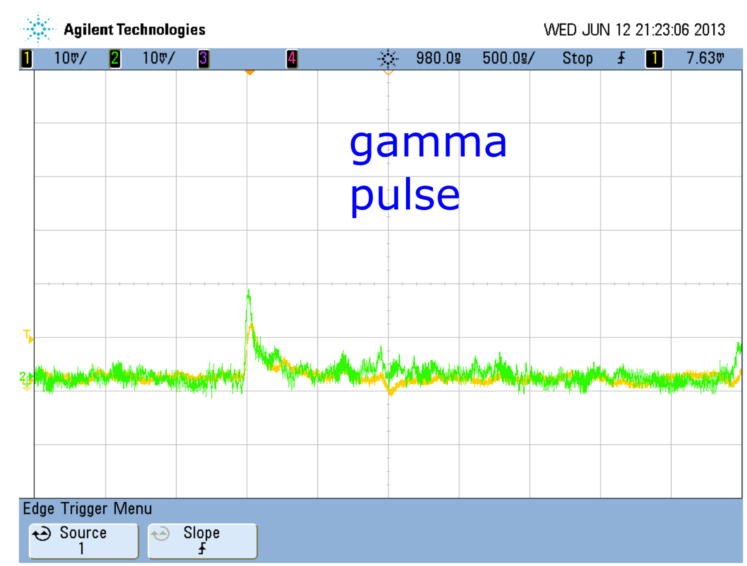

Counting rate [Hz]	no source	^{60}Co in contact [40 kBq]	^{252}Cf in contact [37 kBq]
Delayed trigger, Ch0 ∩ Ch1	0.01	0.01	8.61

Poster ID 40 – Alexander Ivashkin (INR RAS) et al
Development of large size ZnS(Ag)/LiF neutron detector with dual SiPM readout

Subject: thermal neutron detection by sandwich (1x20cm^2 wide):
thin scintillator (ZnS(Ag)/LiF) bars // light guide + dual light readout w/ SiPM

Results: 1) robust neutron signal (~25 ph.electrons per side)
2) effective noise reduction by signal shaping + threshold + coincidence
→ expected high neutron detection efficiency (50% w/ two LiF layers)

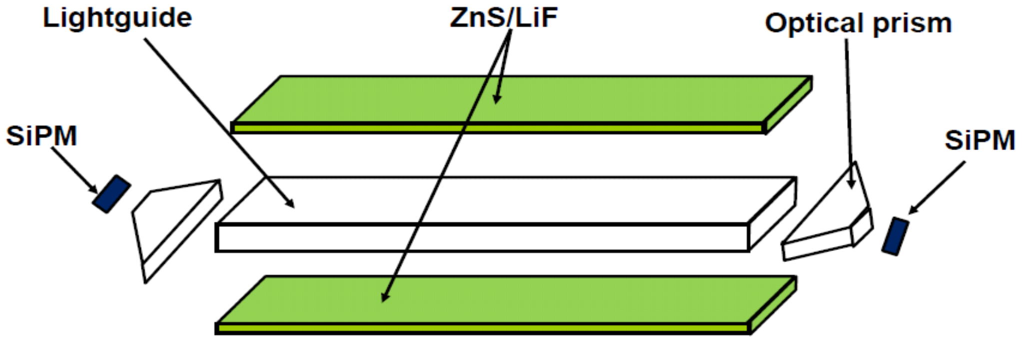

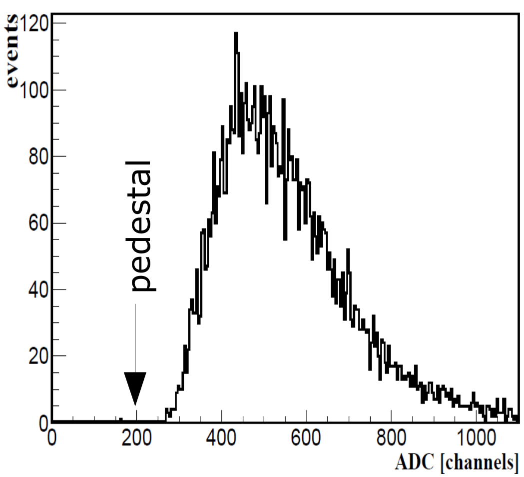

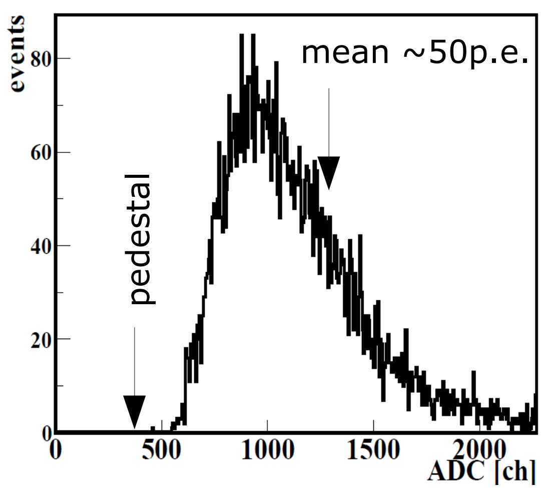

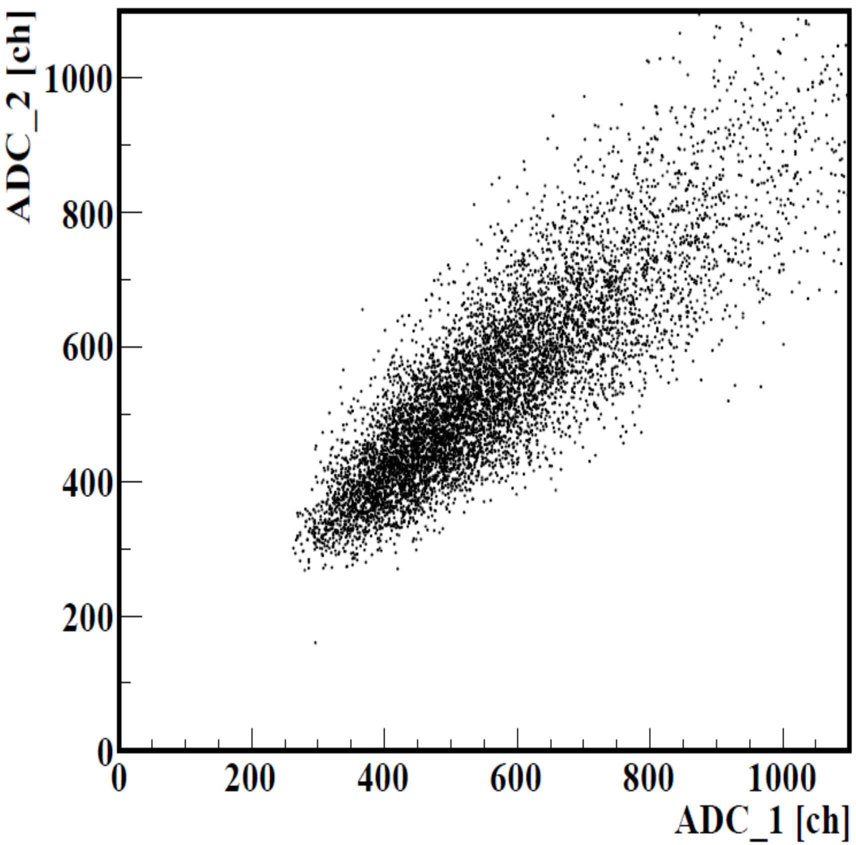

Poster ID 58 – Dmitry Mironov et al
SiPM direct readout of scintillation tiles

Subject: scintillator tile readout with SiPM for the ILC AHCAL → 10^7 tiles 30x30x3 mm
Note: Direct light readout (without WLS-fiber) is critical in terms of response uniformity
Results: SiPM positioned in the center of tile and dimple milled in front of SiPM
→ 13 photo-el./MIP + uniformity better than 8% + tile-tile crosstalk ~2.5%
→ possible scintillator sandwich of scintillator planes

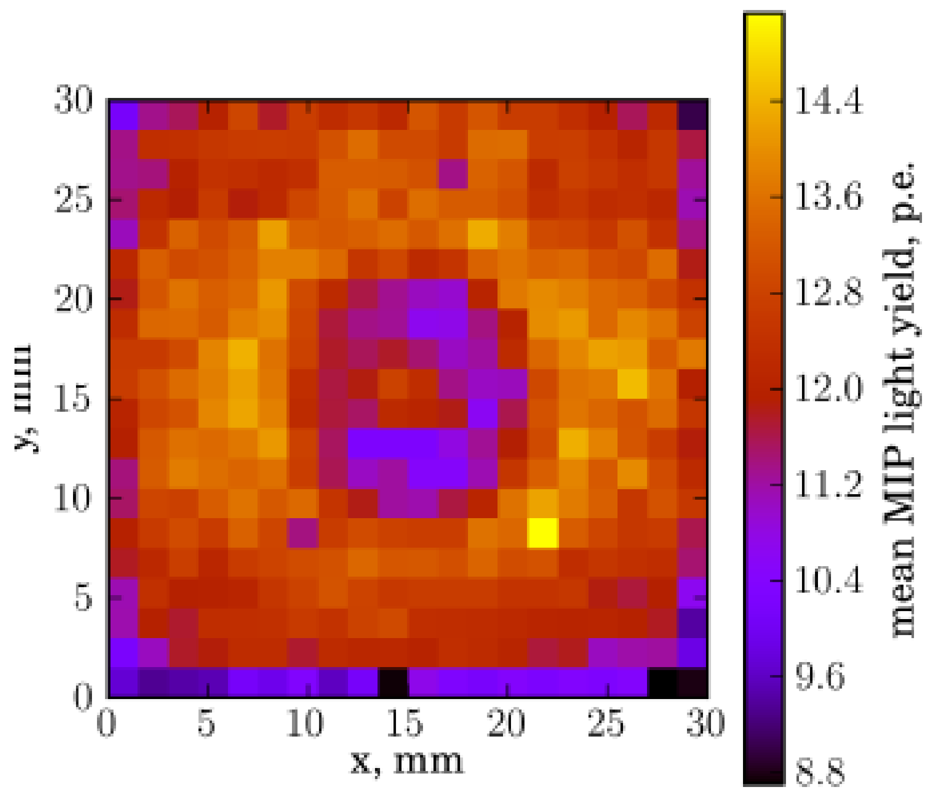

Poster ID 64 – Ryotaro Honda (Tohoku Univ.) et al
A Beam position fiber counter with scintillation fibers and MPPC for high intensity beam handling

Subject: high intensity beam monitor (position and time structure)

Results: - key elements: precision frame for fibers + precision soldering SiPM on PCB
- readout: ADC (EASIROC + bias SiPM) + TDC (on FPGA)
1) position resolution <190μm with high degree of uniformity
2) time resolution <700ps and detection efficiency >97% up to 10MHz rate

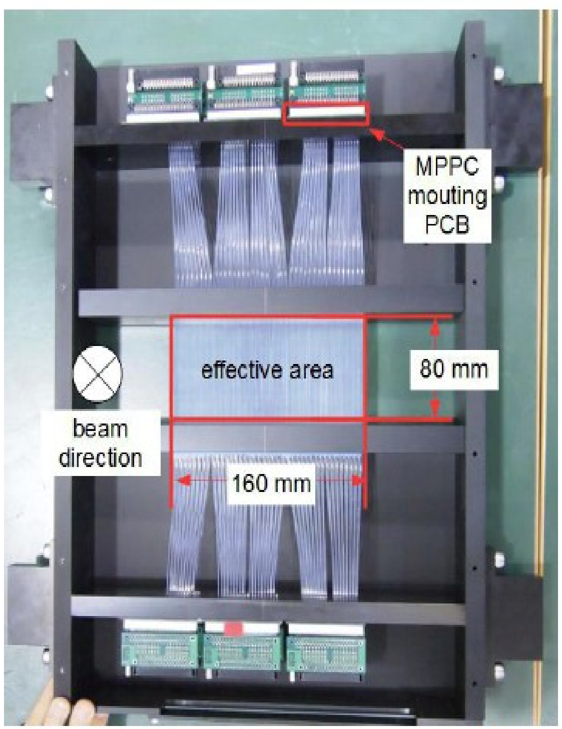

Fig.1. A picture of the beam position fiber counter.

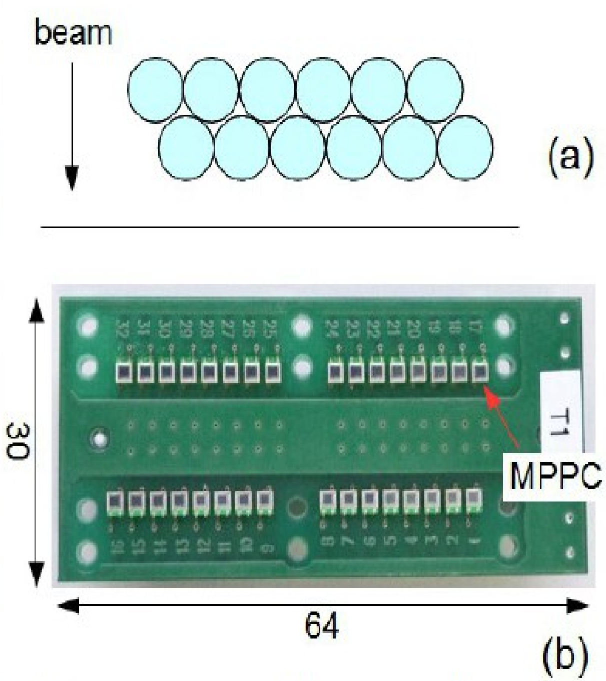

Fig.2. Arrangement of fibers (a) and a picture of MPPC mounting PCB (b).

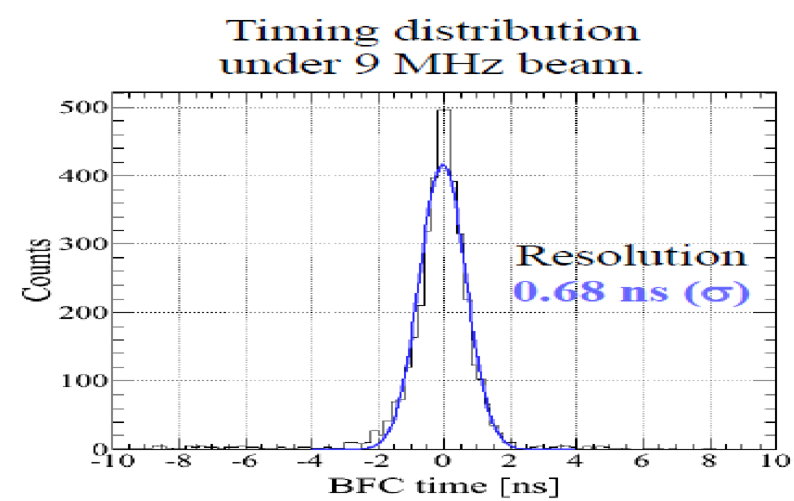

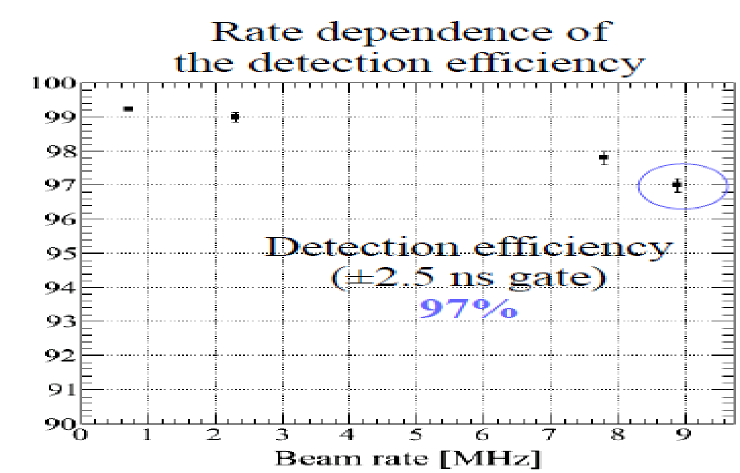

Poster ID 67 – Hyojung Hyun (Kyungpook Univ.) et al

Performances of the Photo-Diode Detectors for the T/BCD of the ISS-CREAM Experiment

Subject: Photo-Diode matrix reading out plastic scintillator planes for e/p separation and triggering in cosmic ray experiment on ISS

Results: - key elements: 20x20 array of 2.3x2.3cm^2 Si PD (full depletion)
- readout: 32 ch. VA-TA chip (Qamp + high dyn. range S/H). Epoxy connect. w/ PCB
1) PD characterization + full system signal/noise measurement
2) Thermal-Vacuum tests of whole flight module + Vibrational tests
→ ready for integration in ISS-CREAM

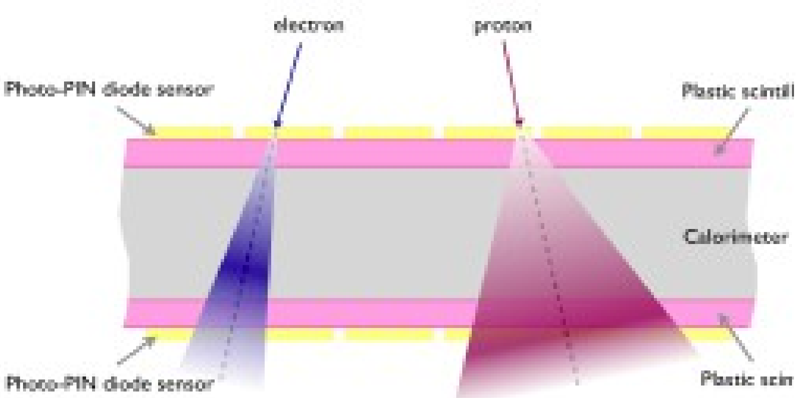

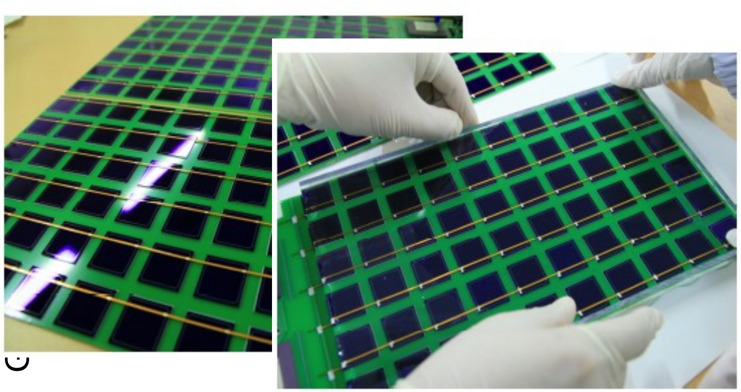

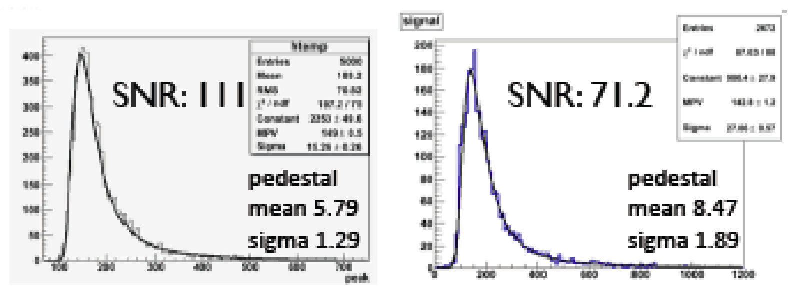

Signal-to-noise ratio measurement result by using 90Sr radioactive source (left) and cosmic ray muons (right)

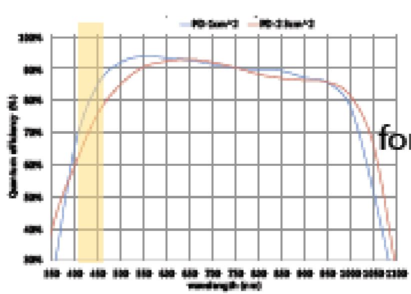

60 ~ 75 %
for the wavelength range from 400 to 450 nm

Quantum efficiency

BCD in X-axis vibration test

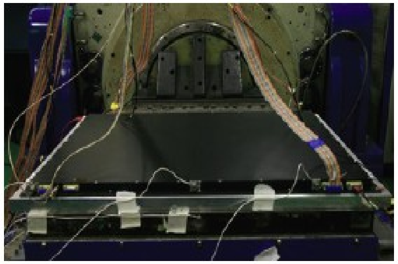

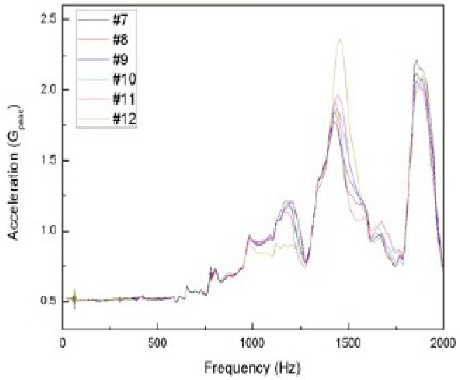

Devices and properties of SiPM/SPAD

Devices and characterization
- SiPM devices/ new features
- VUV sensitivity and cryogenic characterization
- Characterization vs models / simulations

Timing properties
- intrinsic timing
- timing performances in applications

Systems – Applications using SiPM

Cherenkov (RICH, Cherenkov Telescope camera)
Scintillators (crystals, neutron det., plastics)

Other Photo-detectors / Systems

Poster ID 79 – Mikhail Bryushinin (IPTI) et al

Detection of phase- and frequency-modulated optical signals using dynamic space-charge gratings in GaAs, Bi12TiO20 and SiC crystals

Subject: Detection of frequency- and phase-modulated signals with applications in interferometric vibrometers and velocimeters and in photo-conductive and photo-refractive material characterization

Results: 1) demonstration and characterization of pulse response resulting on dynamic space charge gratings from linear frequency modulation (LFM) of interfering beams
2) application: object unif. accelerating results in LFM → pulse shape yields measurement of both velocity and acceleration of object
3) discussion about photo-conducivity of crystals for non steady-state photo-EMF applications

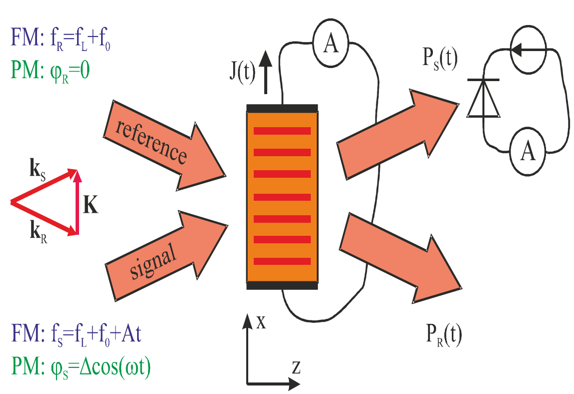

Fig. 1. Scheme of excitation of the non-steady-state photo-EMF and two-wave mixing signals in photoconductive and photorefractive crystals.

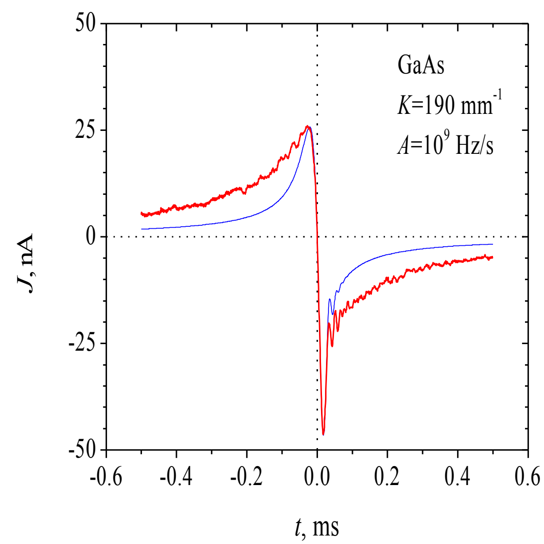

Fig. 2. Pulse response of the GaAs adaptive detector to the frequency-modulated optical signal. λ=633 nm, I_0=240 mW/cm^2.

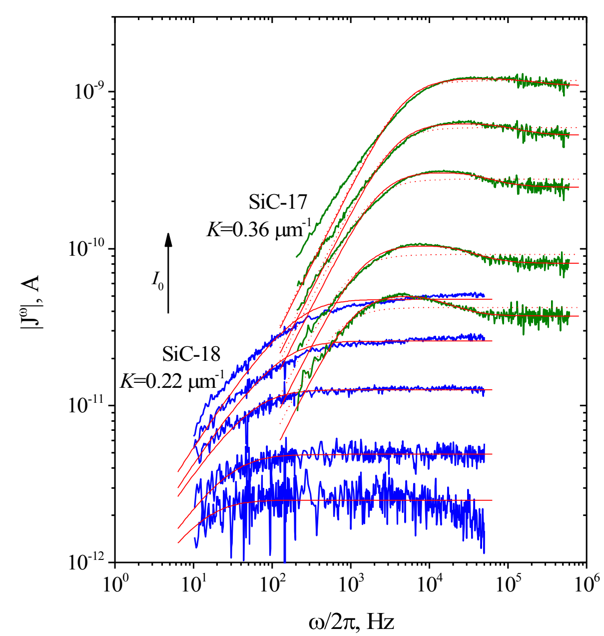

Fig. 3. Frequency transfer functions of the non-steady-state photo-EMF in SiC detectors preliminarily irradiated by reactor neutrons. λ=532 nm, I_0= 110, 210, 540, 1100, 2200 mW/cm^2.

Poster ID 76 – Janna Dokholyan (SEUA) et al
Novel Semiconductor Optical Analyzer

Subject: development of a spectrophotometer based on innovative silicon photo-detector
Results: 1) development of new type of photo-detector selectively sensitive to the radiation spectrum, composed of a n-p Si junction and a n-doped Si Schottky barrier
2) development of an algorithm for disentangling the spectral components of the impinging light based on the analysis of the measured photo-current vs bias voltage
3) development of a compact spectro-photometer sensitive in the range 250-900nm

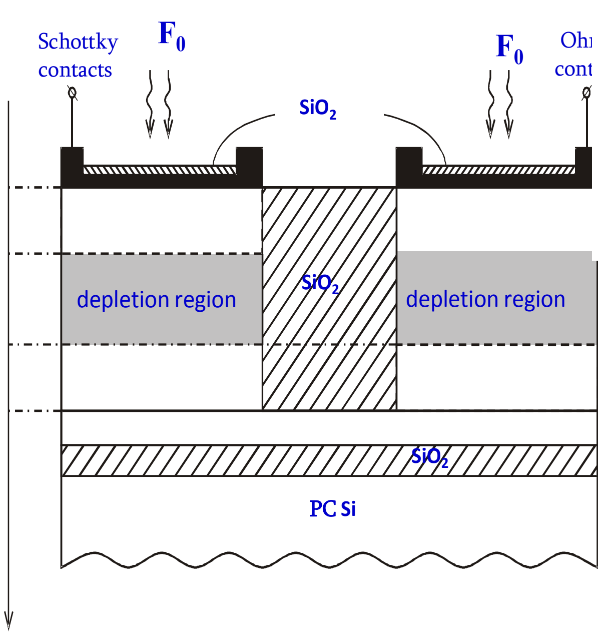

Structure of bipolar photodetector FD-20-30b

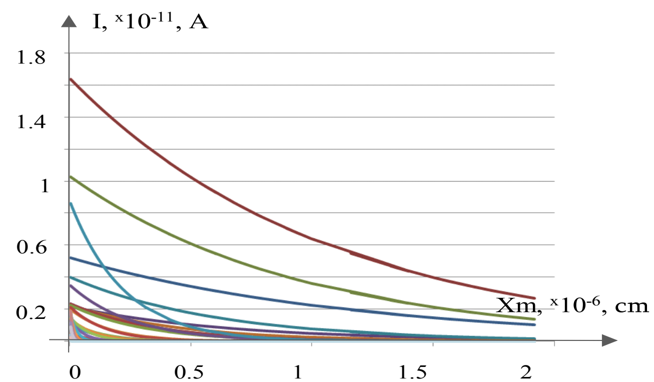

Photocurrent dependences of consistently defined waves on the Xm

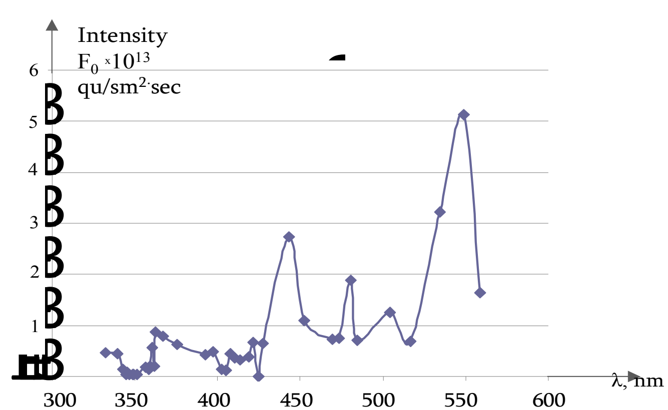

Spectral distribution of radiation intensity

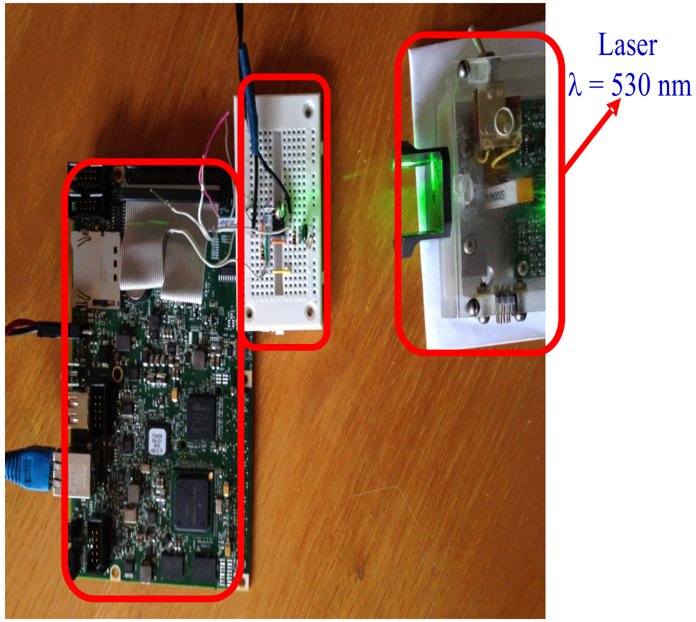

→ Continue enjoying
Poster Session "Blanc" !